ISENTHALPIC THROTTLING (FREE EXPANSION) AND THE JOULE-THOMSON COEFFICIENT

Charles R. Koppany, PhD, Chem. Eng.

January 2, 2014

ISENTHALPIC THROTTLING (FREE EXPANSION) AND THE JOULE-THOMSON COEFFICIENT

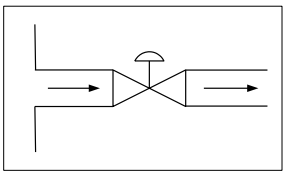

This paper is presented in four major sections. In Section I we discuss the four basic operating regions in which isenthalpic throttling or free expansion of a pure fluid can take place. In Sections II through IV, a fairly comprehensive study of the Joule-Thomson coefficient is conducted. An attempt is made to develop a generalized graphical correlation for the JT inversion curve for pure fluids within the framework of the law of corresponding states.

The three-constant corresponding states equation of Miller (11) provides a very good overall or average representation of the inversion loci for light non polar gases. In addition, an assessment is made of the accuracy of several closed-cubic equations of state for predicting the JT coefficients for nitrogen and carbon dioxide. The four equations tested were:

1. van der Waals equation
2. Redlich-Kwong equation
3. API (modified) Soave equation
4. Peng-Robinson equation

Of the four equations tested, the Redlich-Kwong equation provided the best overall predictions of the JT coefficients for gaseous nitrogen and for both gaseous and liquid carbon dioxide. The overall statistical deviations or trends are summarized in Tables 5, 7 and 8.

Throughout this paper, eight numerical illustrations are given which depict typical computations involving free isenthalpic expansion, the determination of the Boyle temperature and inversion temperature(s) for nitrogen from virial coefficient data, and the calculation of the inversion point and JT coefficients from a typical set of isenthalpic T vs. P data for gaseous ethylene.

Table of Contents

List of Diagrams, Figures, and Tables

ISENTHALPIC THROTTLING (FREE EXPANSION) AND THE JOULE-THOMSON COEFFICIENT

I. Isenthalpic Throttling (Free Expansion)

Introduction The unrestricted expansion of a gas is known as free expansion. For the specific conditions where no work is done, no heat is transferred, and there are essentially no kinetic or potential energy effects, the total energy balance reduces to,

$$\Delta H = 0 \qquad (1)$$

For this specialized case, no change in the system enthalpy is realized. Free flow of a fluid across a valve approximates this process very closely. Some industrial applications of an expansion or throttling process would be in the cooling or liquefaction of gases.

Joule-Thomson Coefficient The Joule-Thomson (Lord Kelvin) coefficient is defined precisely as the differential change in temperature with respect to a differential decrease in pressure under isenthalpic (constant H) conditions. This coefficient is expressed as,

$$\mu_{JT} = \left(\frac{\partial T}{\partial P}\right)_H \qquad (2)$$

It is related to the P-V-T properties of a fluid by the exact relations,

$$\mu_{JT} = -\frac{1}{C_p}\left[V - T\left(\frac{\partial V}{\partial T}\right)_P\right] = -\frac{1}{C_P}\left[V + T\frac{\left(\frac{\partial P}{\partial T}\right)_V}{\left(\frac{\partial P}{\partial V}\right)_T}\right] \qquad (3)$$

The directional change in the temperature when the pressure is decreased ($dP < 0$) across a valve is dictated by the algebraic sign of the JT coefficient. In summary,

Sign of μ_{JT}	Result in dT (for $dP < 0$)
+	$dT < 0$, fluid cools upon expansion
-	$dT > 0$, fluid warms upon expansion
0	$dT = 0$, no temperature change (inversion point)

For the special case of an expanding ideal gas, Equation 3 reduces to,

$$\mu_{JT} = 0 \qquad (4)$$

For an ideal gas no temperature change is realized in any case. However, this is not strictly true if there is an appreciable change in kinetic energy across the valve or flow passage. For instance, if an ideal gas is flowing from a large reservoir and expands immediately across a valve situated in the exit pipe line, then the total energy balance written across the valve becomes,

$$\Delta H + \Delta(KE) = \Delta H + \frac{u^2}{2g_c} = 0 \qquad (5)$$

where u is the fluid velocity prevailing at the valve exit.

In Sections II through IV a more comprehensive treatment of the JT coefficient will be given. An attempt is made to develop a generalized inversion curve for fluids within the framework of the Law of Corresponding States. In addition, an assessment is made as to how accurate several cubic equations of state are for predicting JT coefficients for nitrogen and carbon dioxide.

Regions of Isenthalpic Throttling Figures 1 through 5 illustrate four basic operating regions of special interest which are displayed on H versus T diagrams for the isenthalpic throttling ($\Delta H = 0$) of a pure fluid. The first case (Figure 1) represents the situation where a superheated vapor is throttled from state 1 down to a lower pressure (state 2) such that the enthalpy lies above the saturated vapor locus during the entire traverse. It should be pointed out here, that each end point reached is presumed to be at an equilibrium state i.e. sufficient time has elapsed for the final state of the system to reach equilibrium. If an equation of state or CS correlation is being used to calculate T_2, a trial and error procedure is involved. The value of T_2 is varied until the criterion $\Delta H = 0$ ($H_1 = H_2$) is satisfied. For this entire traverse, the sign of the Joule-Thomson coefficient is positive i.e. the temperature continually decreases as the pressure decreases.

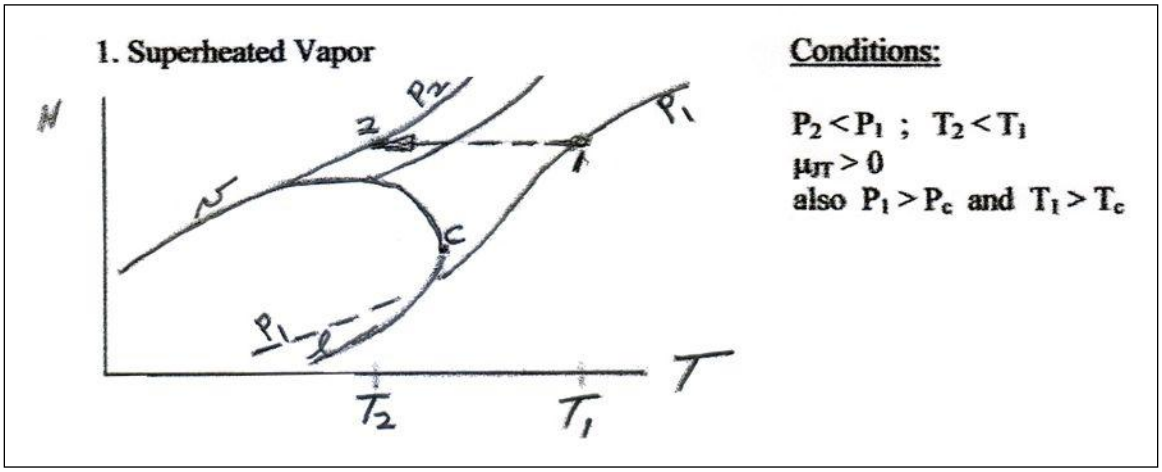

Figure 1. Region 1 of Isenthalpic Throttling ($\Delta H=0$) for a Pure Fluid.

In the second case (Figure 2), the fluid is throttled from state 1 directly into the two-phase region (state 2). The value of H_1 lies below the saturated vapor locus at P_2, T_2^{sat}. In other words, P_2 is

the saturation (vapor) pressure of the fluid at T_2. The determination of T_2 therefore does not require an iterative calculation. The final state or quality x (wt. fraction vapor) of the fluid is readily computed by a simple enthalpy balance, Equation 6 below,

$$H_1 = H_2 = x H_2^{SV} + (1-x) h_2^{SL} \qquad (6)$$

As in case 1, a temperature decrease is also effected upon expansion, and the JT coefficient is still positive.

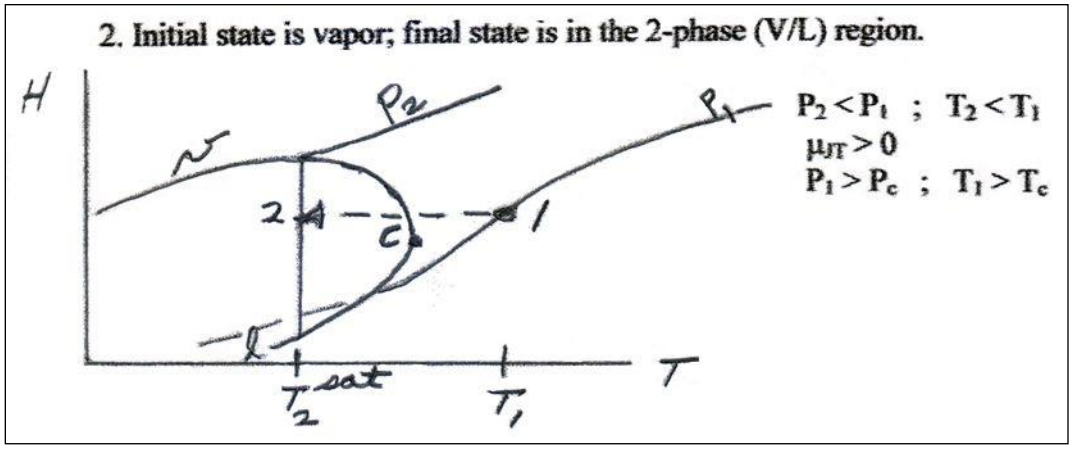

Figure 2. Region 2 of Isenthalpic Throttling (ΔH=0) for a Pure Fluid.

The third case illustrated on Figure 3 involves a high temperature vapor where the high pressure lines intersect and then, at higher temperatures, lie above the ideal gas (P = 0) and lower pressure lines. As the pressure is continually decreased at constant H from state 1, say P_1 = 2500 psia, to lower and lower pressures P_2, the temperature increases. In this operating region, the sign of the JT coefficient is negative. This behavior is readily observed for gaseous nitrogen above a temperature of 570 deg. F.

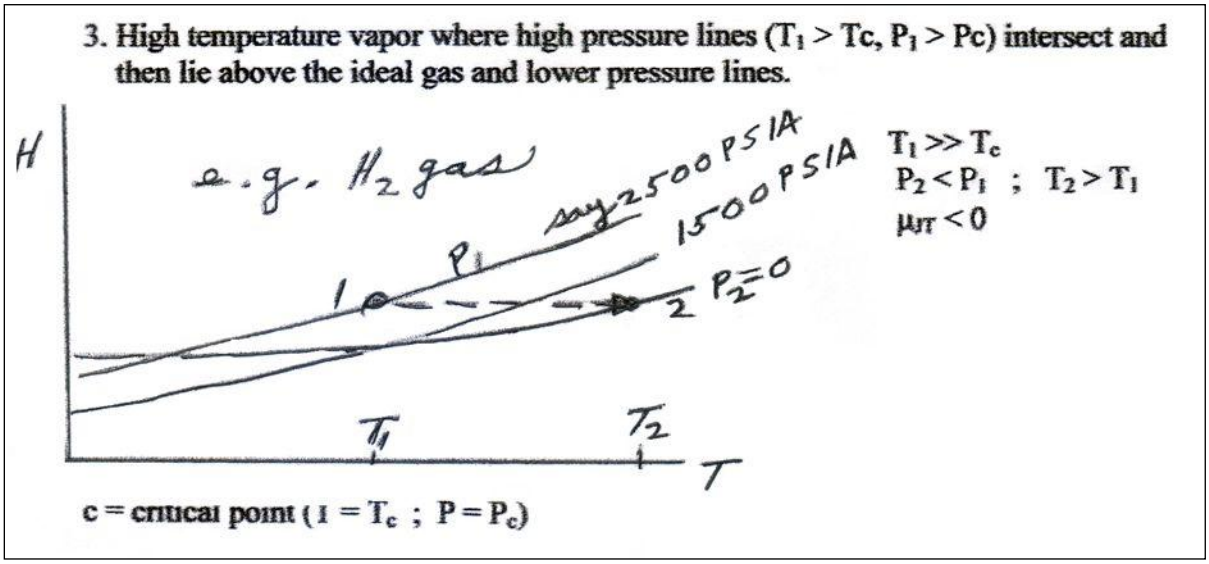

Figure 3. Region 3 of Isenthalpic Throttling (ΔH=0) for a Pure Fluid.

In the fourth and final case (Figure 4), we start out with a high pressure (compressed) liquid (state 1) at a temperature generally well below the critical temperature. As the pressure is lowered at constant H, the liquid is gradually decompressed until the saturated liquid locus is reached. During this process, the temperature increases. At Point 2, on the saturated liquid locus, the temperature will reach a maximum value T_2^{sat}. As the pressure is decreased further from this point, the temperature drops continually, and the two phase region is entered. Point 3 would be a typical example. The fluid continues to flash more and more as the pressure and temperature are further diminished at constant H ($H_1 = H_2 = H_3$) and so on. At any point in the two phase region, Equation 6 can, once again, be used to calculate the stream quality.

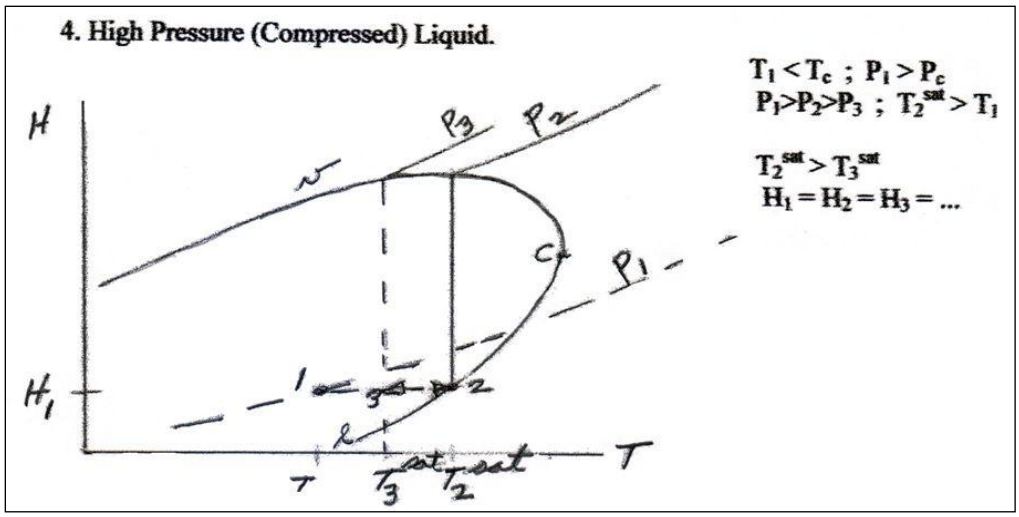

Figure 4. Region 4 of Isenthalpic Throttling (ΔH=0) for a Pure Fluid.

A qualitative plot of T versus P for this process, as illustrated in Figure 5, will display a point of maximum temperature at T_2, P_2^{sat}. To the right of this point, the fluid exists as a compressed liquid. To the left, it exists as a two-phase V/L fluid.

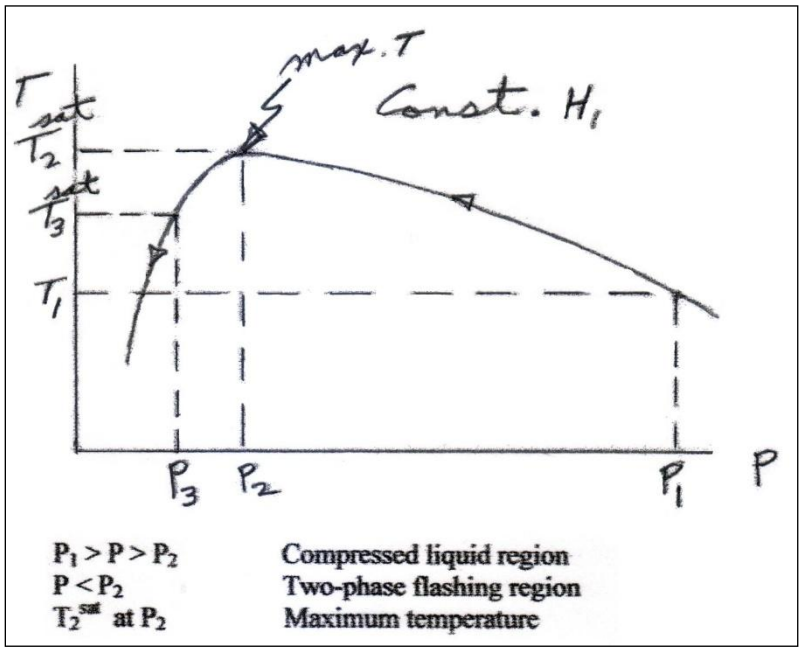

Figure 5. Qualitative plot of T versus P for region 4 of Isenthalpic Throttling (ΔH=0) for a Pure Fluid.

Two-Phase Region When Equation 6 is solved explicitly for the stream quality,x, it becomes,

$$x = \frac{V}{F} = \frac{H_1 - h_2^{SL}}{H_2^{SV} - h_2^{SL}} \qquad (7)$$

Each of the enthalpy terms in Equation 7 can readily be calculated using a set of Corresponding States charts such as those of Lee and Kesler (1) or from an available equation of state. With the aid of a corresponding states chart each of the enthalpy terms above would be computed from the following expressions:

$$H_1 = H_1^o - RT_C\left(\frac{H_1^o - H_1}{RT_C}\right) \qquad (8)$$

$$H_2^{SV} = H_2^o - RT_C\left(\frac{H_2^o - H_2^{SV}}{RT_C}\right) \;;\; h_2^{SL} = H_2^o - RT_C\left(\frac{H_2^o - h_2^{SL}}{RT_C}\right) \qquad (9a,b)$$

H_1^o and H_2^o represent the reference state ideal gas enthalpies for the inlet and outlet streams undergoing the isenthalpic process in question. The terms in brackets represent the isothermal departure with pressure of the stream enthalpy from the ideal gas state. Below, we first describe the Lee-Kesler CST method for calculating stream enthalpy departures, and then we address the procedure used for computing ideal gas reference enthalpies.

Three-Parameter CS Correlation In a series of three papers Pitzer and Curl (2,3,4) showed that the compressibility factor, the second virial coefficient and other thermodynamic property departure functions could adequately be represented at constant Tr and Pr by a linear function of the acentric factor, ω. They proposed that any of the above stated properties, e.g. the compressibility factor Z, could be correlated by a functional relationship of the form,

$$Z = Z^{(o)} + \omega Z^{(1)} \qquad (10)$$

where $$Z^{(o)} = f_1(T_r, P_r)\;;\; Z^{(1)} = f_2(T_r, P_r) \qquad (11a,b)$$

$Z^{(o)}$ is the compressibility factor for simple (spherical) fluids and $Z^{(1)}$ is the compressibility factor contribution due to the departure from sphericity or simple fluid behavior. $Z^{(o)}$ and $Z^{(1)}$ are presented as separate charts or tables. Generally speaking, the Curl-Pitzer correlation covers the operating range:

$$T_r = 0.8 \text{ to } 4.0 \text{ and } P_r = 0 \text{ to } 9.0$$

Both the vapor and liquid regions are covered.

Nearly 20 years later Lee and Kesler (1) improved upon the Curl-Pitzer correlation for the following regions of application:

1. the critical region
2. low-temperature liquids
3. wide-boiling mixtures
4. and extended the temperature and pressure limits to T_r from 0.3 to 4 and P_r from 0 to 10.

Like Curl and Pitzer did, Lee-Kesler developed a graphical/tabular correlation for the compressibility factor, enthalpy departure, entropy departure, isobaric heat capacity departure and fugacity coefficient within the framework of three parameter CS theory.

The enthalpy departure function is expressed in the following format:

$$\frac{H^o - H}{RT_c} = \left[\frac{H^o - H}{RT_c}\right]^{(o)} + \frac{\omega}{\omega_r}\left[\left(\frac{H^o - H}{RT_c}\right)^{(r)} - \left(\frac{H^o - H}{RT_c}\right)^{(o)}\right] \quad (12)$$

or

$$\frac{H^o - H}{RT_c} = \left[\frac{H^o - H}{RT_c}\right]^{(o)} + \omega\left[\frac{H^o - H}{RT_c}\right]^{(1)} \quad (13)$$

The authors provide similar type expressions for the entropy and isobaric heat capacity departure functions. In Equation 12, the groupings in brackets designated by superscripts (o) and (r) were correlated via a modified BWR equation of state. Superscript (o) refers to simple fluids and superscript (r) to a reference fluid. Both of the departure functions for the three thermodynamic properties plus the compressibility factor are calculated from a reduced form of the Benedict-Webb-Rubin or BWR equation. Lee and Kesler performed a multi-property fit and arrived at one set of BWR constants (12 total) for simple fluids and another set of 12 for the reference fluid. n-octane with $\omega^r = 0.3978$ was chosen as the heavy reference fluid since it is the heaviest hydrocarbon for which there are accurate PVT and enthalpy data existing over a wide range of conditions.

The data used to determine the simple fluid constants for the modified BWR equation were principally for Ar, Kr and methane ($\omega \cong 0$). The authors present separate tables and charts for each of the thermodynamic property functions for T_r from 0.3 to 4 and for P_r from 0 to 10. Figure 6 and Figure 7 shown here provide plots for the enthalpy departure functions designated in Equation 13 as a function of T_r and P_r. They will be used in an illustration to be given later in this section.

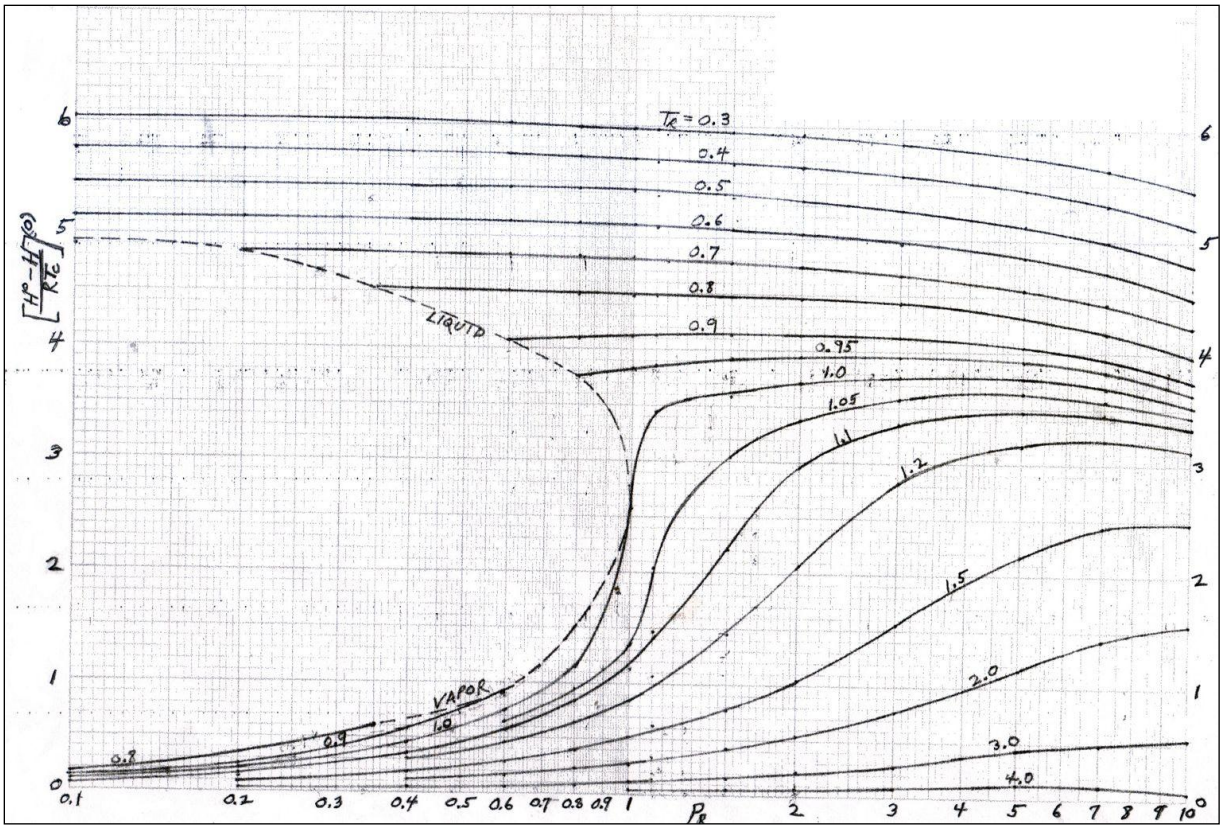

Figure 6. Simple Fluid Term - Enthalpy Pressure Effect.

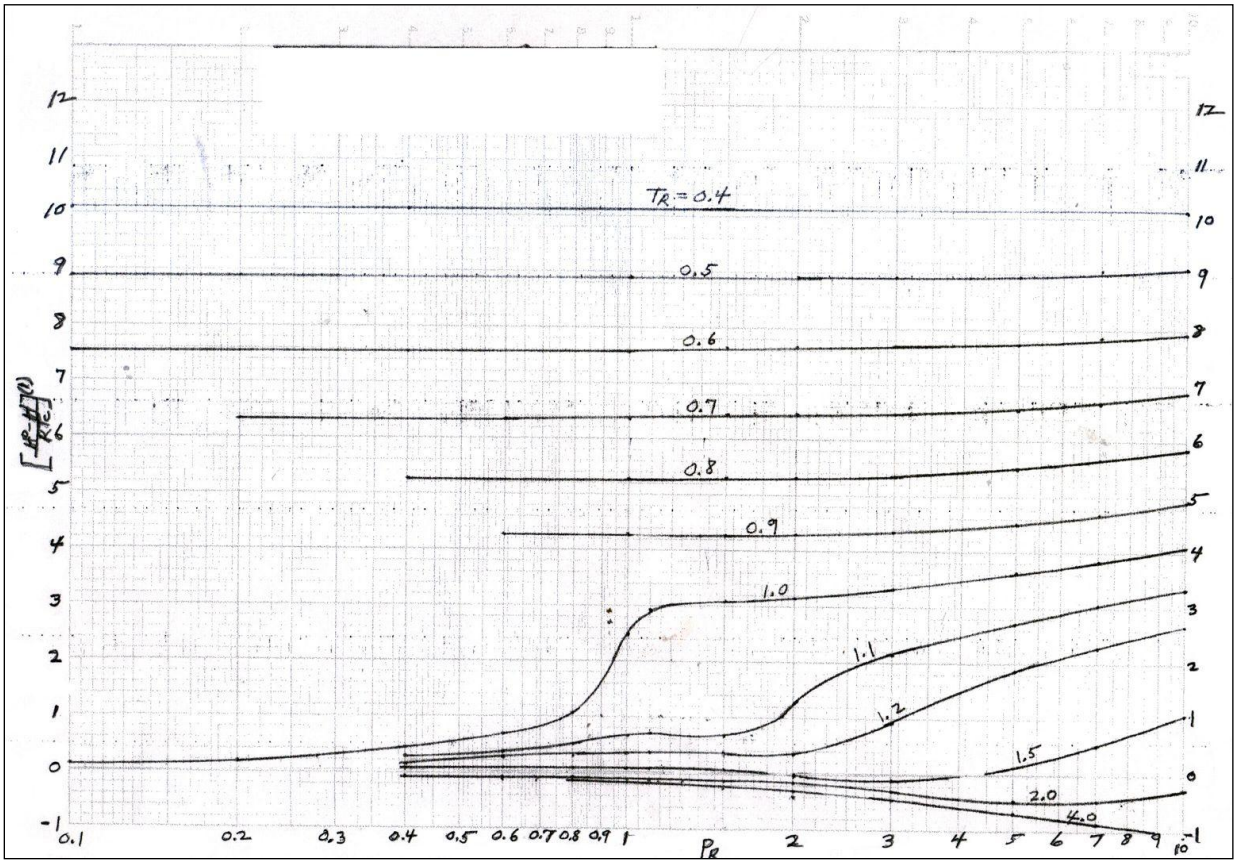

Figure 7. Real Fluid Term - Enthalpy Pressure Effect.

Ideal Gas Reference Enthalpy Generally speaking, it is desirable to evaluate or express enthalpy relative to some base or reference level. Procedure 7A1.1 of the Data Book of the American Petroleum Institute (5) provides a thermodynamically consistent set of equations for this purpose. These expressions consist of polynomial fits in temperature and are as follows:

$$For\ enthalpy: \qquad H^o = A + BT + CT^2 + DT^3 + ET^4 + FT^5 \qquad (14)$$

$$For\ C_p: \qquad C_p^o = \frac{d\,H^o}{d\,T} = B + 2CT + 3DT^2 + 4ET^3 + 5FT^4 \qquad (15)$$

$$For\ entropy: \qquad S^o = B\,LnT + 2CT + \frac{3}{2}DT^2 + \frac{4}{3}ET^3 + \frac{5}{4}FT^4 + G \qquad (16)$$

These three expressions are thermodynamically consistent with one another. The various units employed in Equations 14-16 are as follows:

T = temperature in degrees Rankine
H^o = ideal gas enthalpy at T in Btu/Lb
$C_p{}^o$ = ideal gas isobaric heat capacity at T in Btu/Lb-deg. R
S^o = ideal gas entropy at T and at some reference pressure in Btu/Lb-deg. R

The constants A through G are derived coefficients. Procedure 7A1.1 of the API Data Book offers two sets of base levels for enthalpy and entropy. They are:

1. H = 0 for the pure saturated liquid at -200 deg. F and S^o = 1 for the ideal gas at 0 deg. R and 1 psia reference pressure.

2. H^o = 0 for the ideal gas at 0 deg. R and S^o = 0 for the ideal gas at 0 deg. R and a reference pressure of 1 atm.

The coefficients B through F are the same for both datum sets. However, A and G are different for any given component. An abridged list of coefficients for the second base level set is provided in Table 1 for some of the more common hydrocarbons and inorganic gases. The second base level is used in the illustrations to follow.

The Total Energy Balance Before proceeding any further here let us review the nature of the total energy balance. For the general case of steady state flow of a fluid flowing through a hydraulic network, the total energy balance can be written as,

$$H_2 - H_1 + \frac{u_2^2 - u_1^2}{2g_c} + \frac{g}{g_c}(z_2 - z_1) = Q - W_s \qquad (17)$$

This equation relates the changes in enthalpy, kinetic and potential energies between states 1 and 2 of the flowing system to the net exchange of heat and mechanical shaft work between flowing system and its surroundings. Below are given some special applications of Equation 17.

1. For the case of either a nozzle, venturi meter or orifice, a significant change in fluid velocity is incurred because of a change in cross-sectional area of the accompanying piping, without any shaft work or heat being transferred.. For horizontal flow, we would then have,

$$H_2 - H_1 + \frac{u_2^2 - u_1^2}{2\,g_c} = \Delta H + \frac{u_2^2 - u_1^2}{2\,g_c} = 0 \qquad (18)$$

2. For the case of a compressor or turbine situated in the network, the change in kinetic energy is normally very small with the process being almost perfectly reversible adiabatic. For horizontal flow, once again,

$$H_2 - H_1 = -W_s \qquad (19)$$

3. In the case of a heat exchanger, the process is essentially conducted isobarically with negligible kinetic and potential energy changes and no shaft work being performed. The total energy balance then reduces to,

$$H_2 - H_1 = \Delta H = Q \qquad (20)$$

4. For an expansion or throttling valve, the fluid has a very small initial velocity with any velocity attained being almost immediately dissipated into internal energy after passage through the valve. Because of the rapidity of the process, no shaft work or heat is transferred, and for a horizontal configuration we would have,

$$\Delta H = H_2 - H_1 = 0 \;\; or \;\; H_1 = H_2 \qquad (21)$$

For steady state flow, fluid velocity changes due to changes in cross-sectional flow area or pipe diameter and fluid density variation are accounted for via the <u>continuity equation</u>,

$$W = mass\ flow rate = u_1 A_1 \rho_1 = u_2 A_2 \rho_2 \qquad (22)$$

where ρ is the fluid density or reciprocal of the fluid specific volume ($\rho = 1/v$).

Illustration 1 An ideal gas flows through a valve where the pressure is reduced from 10 to 2 atm abs. The surrounding temperature and high pressure gas are at 25 deg. C. The gas velocity is 10 ft/sec and is essentially the same on either side of the valve. What is ΔH through the valve and the gas temperature at the valve exit ?

This expansion process occurs very rapidly. As a result, there is basically no heat transfer between the system (gas) and surroundings. No work is done along with no change in kinetic energy across the valve ($u_1 = u_2$). Then, if we presume that the flow is completely horizontal, the total energy balance reduces to,

$$\Delta H = 0$$

Since the flowing gas is a perfect gas with no change in enthalpy, ΔT = 0, and the downstream temperature is 25 deg. C.

Illustration 2 A stream of ideal gas at 700 deg. R exits a large tank and immediately enters a valve situated in the exit pipe line. In the process of flowing through the valve, the gas is accelerated horizontally and adiabatically from rest to 1600 ft/sec.

a) Write the form of the total energy balance that applies in this case.

b) What is the temperature of the gas at the valve exit ?

Gas properties: C_p = 7 Btu/Lbmole- deg. R , MW = 29

Part a:

For this case, there a very significant change in kinetic energy across the valve with $Q = W_s = 0$. Therefore, the total energy balance reduces to Equation 8.89,

$$\Delta H + \frac{\Delta u^2}{2 g_c} = H_2 - H_1 + \frac{u_2^2 - u_1^2}{2 g_c} = 0 \quad where \;\; u_1 = 0$$

Part b:

$$Then\ we\ have \qquad \Delta H + \frac{(1600)^2}{(2)(32.16)(778)} \frac{Btu}{Lb} = 0$$

$$Solving\ for\ \Delta H\ we\ get \qquad \Delta H = H_2 - H_1 = -51.16 \frac{Btu}{Lb}$$

$$Or \qquad \Delta H = -(51.16)(29) = -1483.6 \frac{Btu}{Lbmole}$$

$$Since\ the\ gas\ is\ ideal, \qquad \Delta H = C_P (T_2 - T_1) = -1483.6 \frac{Btu}{Lbmole}$$

Now the valve exit temperature can be readily computed,

$$T_2 - 700 = \frac{-1483.6}{7} = -211.9$$

$$Or \qquad T_2 = 488 \deg.R = 28 \deg.F$$

Illustration 3 Ethylene gas (dense fluid) flowing in a pipeline at 60 deg. F and 1000 psia enters an expansion valve where the pressure is suddenly reduced to 200 psia. It is required to estimate the valve exit temperature and the state of the exit fluid. If it turns out that the exit fluid is in the state of two phases (V+L), what would be the stream quality (wt % vapor present) ? For ethylene, over the temperature range of – 100 deg. F to the critical, the vapor pressure is well represented by the Antoine relation:

$$Ln\, P_{VP} = 13.38425 - \frac{3861.566}{T + 519.7205} \quad with\ T\ in\ \deg.F\ and\ P_{VP}\ in\ psia.$$

Two procedures will be employed and the results compared:

a) Use of the generalized Lee-Kesler CS charts for computing enthalpies (Figures 6 and 7)

b) Use of the H-T diagram developed specifically for ethylene based on the Peng-Robinson equation.

The following physical properties taken from the Data Book of the American Petroleum Institute (API) will be required for Part a:

$$P_C = 729.8\ psia\ ;\ T_C = 48.58 \deg.F\ (508.28 \deg.R)\ ;\ \omega = 0.0868\ ;\ MW = 28.05$$

Part a: The first step consists of determining whether the exit condition 2 is in the two-phase region or not. Define H_1 as the fluid enthalpy at the valve inlet and h_2^{SL} as the saturated liquid enthalpy and H_2^{SV} the saturated vapor enthalpy, both at the valve outlet pressure. If $h_2^{SL} < H_1 < H_2^{SV}$, then the exit phase condition is definitely two-phase.

If $H_1 > H_2^{SV}$, then the stream is all vapor at the exit. The saturation temperature T_2^{sat} at the specified valve exit pressure P_2 is calculated from the specified VP equation after it is rearranged and solved explicitly for the temperature.

$$T_2^{sat} = \frac{3861.566}{13.38425 - Ln\,P_2} - 519.7205$$

$$T_2^{sat} = \frac{3861.566}{13.38425 - Ln(200)} - 519.7205 = \frac{3861.566}{13.38425 - 5.29832} - 519.7205$$

$$T_2^{sat} = -42.2 \text{ deg}.F$$

The various required enthalpy values are now calculated from the Lee-Kesler CS charts - Figures 6 and 7 and Equation 13.

At the valve inlet, 60 deg. F and 1000 psia,

$$P_{R1} = \frac{1000}{729.8} = 1.37 \quad ; \quad T_{R1} = \frac{60 + 459.7}{508.28} = 1.02$$

Using Equation 14 and the appropriate coefficients for ethylene read from Table 1, the inlet ideal gas enthalpy at 60 deg. F becomes $H_1^o = 155.0$ Btu/Lb based on the API datum of $H^o = 0$ at 0 deg. R. From the Lee-Kesler charts we read,

$$\left[\frac{H^o - H}{RT_C}\right]_1^{(o)} = 3.3 \quad ; \quad \left[\frac{H^o - H}{RT_C}\right]_1^{(1)} = 3.$$

$$\left(H^o - H\right)_1 = \frac{(1.987)(508.28)}{28.05}\left[3.30 + (0.0868)(3.)\right]$$

$$\left(H^o - H\right)_1 = (36.0)(3.56) = 128.2 \; Btu/Lb$$

$$H_1 = 155.0 - 128.2 = 26.8 \; Btu/Lb$$

Saturation enthalpies at outlet:

$$P_{R2} = \frac{200}{729.8} = 0.274 \quad ; \quad T_{R2} = \frac{-42.2 + 459.7}{508.28} = 0.82$$

Also H_2^o = 120.5 Btu/Lb at – 42.2 deg. F.

$$H_2^{SV} = 120.5 - \frac{(1.987)(508.28)}{28.05}\left[0.48 + (0.0868)(0)\right] = 120.5 - (36.)(0.48)$$

$$H_2^{SV} = 120.5 - 17.3 = 103.2 \ Btu/Lb$$

$$h_2^{SL} = 120.5 - (36.)\left(4.6 + (0.0868)(5.)\right) = 120.5 - 181.2 = -60.7 \ Btu/Lb$$

Here it is readily apparent that H_1 (26.8 Btu/Lb) lies between the values of h_2^{SL} = -60.7 Btu/Lb and H_2^{SV} = 103.2 Btu/Lb. Therefore, the final state of the system is two phase (V + L) at – 42.2 deg. F and 200 psia. The exit stream quality can now be computed directly from Equation 7:

$$x_2 = \left(\frac{V}{F}\right)_2 = \frac{H_1 - h_2^{SL}}{H_2^{SV} - h_2^{SL}} = \frac{26.8 - (-60.7)}{103.2 - (-60.7)} = \frac{87.5}{163.9} = 0.534 \ wt.\ fraction\ vapor$$

Part b: Figure 8 and Figure 9 represent H-T diagrams for ethylene. They were developed by this author using a BASIC program which employs the Peng-Robinson equation to compute enthalpy departures. From Figure 8 we located the inlet condition of 60 deg. F and 1000 psia at H_1 = 1038 Btu/Lb. Now by following this value of enthalpy horizontally to the left to a pressure of 200 psia, we enter the two-phase region and wind up at a temperature of – 42 deg. F. At this condition,

$$H_2^{SV} = 1104 \ Btu/Lb \quad ; \quad h_2^{SL} = 947 \ Btu/Lb$$

And then, once again, from Equation 9 we can compute the exit stream quality based on the enthalpy values read from the ethylene H-T chart,

$$x_2 = \frac{1038 - 947}{1104 - 947} = \frac{91.0}{157.0} = 0.580$$

The quality predicted here is slightly higher than that calculated from Lee-Kesler enthalpies.

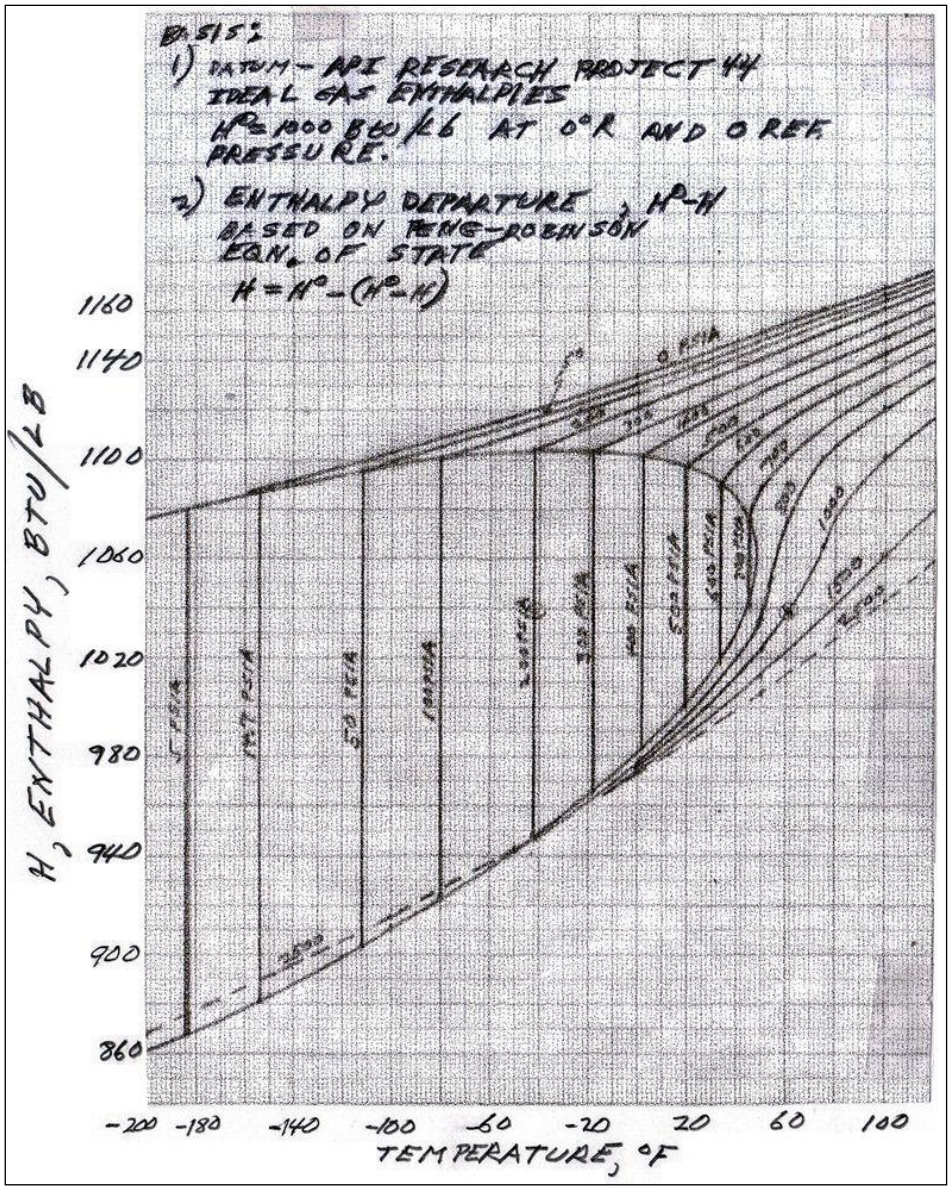

Figure 8. Enthalpy of Ethylene Based on the Peng-Robinson EOS.

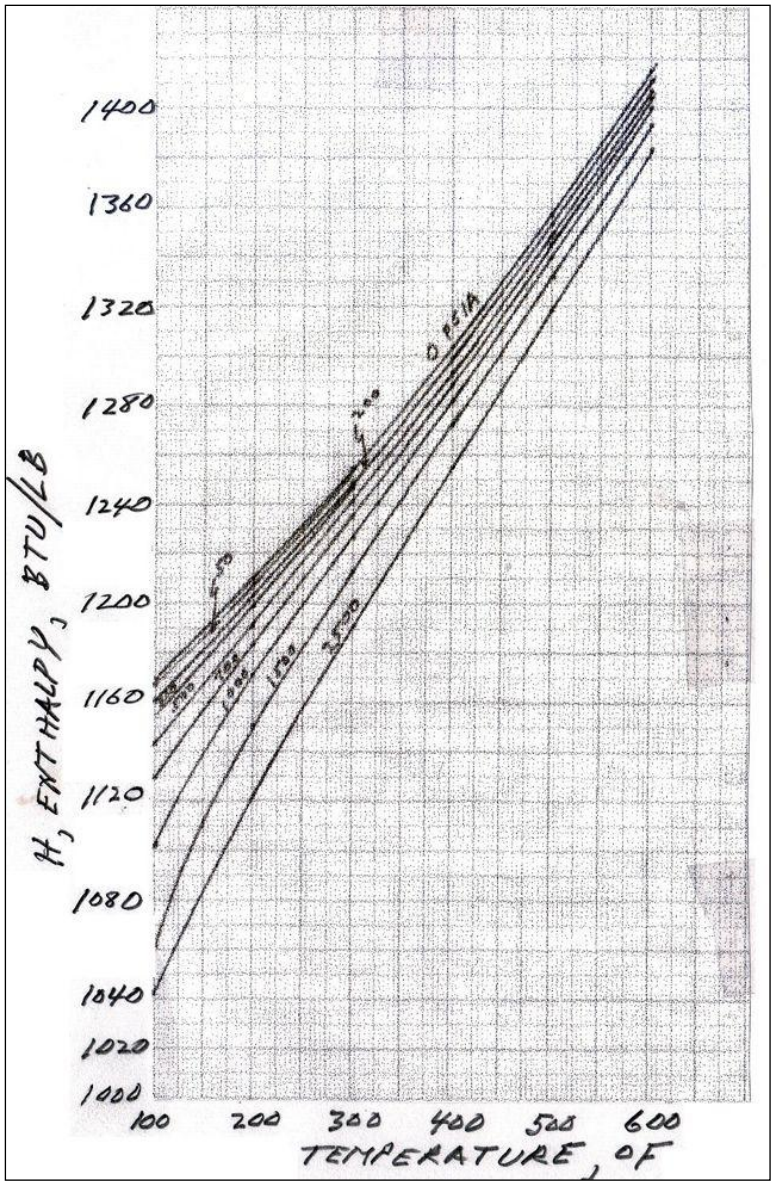

Figure 9. Enthalpy of Ethylene Based on the Peng-Robinson EOS - High Temperature Region.

Illustration 4 An infinite supply of compressed liquid water at 250 deg. F and 6,000 psia is expanded across a valve to lower and lower pressure levels(equilibrium states). After the water is isenthalpically decompressed to such an extent that the condition at the valve exit is a saturated liquid, then a further drop in pressure will produce flashing. Using the Keenan and Keyes steam tables, we wish to establish the temperature-pressure profile for the fluid at the valve exit.

Keenan and Keyes (6), Steam Tables, John Wiley & Sons, 1969 (Table 4, Pages 104-107) provide thermodynamic properties for compressed liquid water from 500 to 20,000 psia. At the valve inlet condition of 6000 psia and 250 deg. F, we read h_1 = 231.19 Btu/Lb. Next a host of lower pressures (valve exit) are selected and the temperatures determined such that $h_1 = h_2$ = 231.9 Btu/Lb. These operations were performed by reading values from Table 4 and using linear interpolation. For example, at P_2 = 4000 psia, we read,

T, deg. F	h_2, Btu/Lb
250	226.93
300	277.15

Then by simple linear interpolation,

$$\frac{T_2 - 250}{300 - 250} = \frac{231.19 - 226.93}{277.15 - 226.93} = \frac{4.26}{50.22}$$

$$Or \qquad T_2 = 254.2 \text{ deg}.F \ at \ 4000 \ psia$$

Similar calculations were performed at the pressure levels of 2000, 1000 and 500 psia to give,

P, psia	T_2, deg. F
2000	258.4
1000	260.4
500	261.4

As the downstream pressure is further diminished, the temperature continually increases to reach a maximum value at the saturated liquid locus. This point was also determined by linear interpolation of the data read from the Steam Tables. On Page 5 (Table 1of the steam tables) we read:

Sat T, deg. F	Sat P, psia	h_2, Btu/Lb
262	36.64	230.79
264	37.89	232.83

$$\textit{Then} \qquad \frac{T_2 - 262}{264 - 262} = \frac{P_2 - 36.64}{37.89 - 36.64} = \frac{231.19 - 230.79}{232.83 - 230.79} = \frac{0.40}{2.04}$$

$$\textit{Solving for } P \textit{ and } T: \qquad T_2 = 262.4 \deg.F \quad \textit{and} \quad P_2 = 36.89 \; psia \;\; (\textit{saturated liquid})$$

At this point, a further decrease in the exit pressure will produce lower temperatures (saturation conditions). For example, at 250 deg. F and 29.82 psia, we read:

$$h_2^{SL} = 218.59 \, Btu/Lb \quad and \quad H_2^{SV} = 1164.2 \, Btu/Lb$$

The stream quality is determined from Equation 7:

$$x_2 = \frac{231.19 - 218.59}{1164.2 - 218.59} = \frac{12.6}{045.6} = 0.0133 \; wt.\, fr.vapor$$

The results of similar calculations at lower saturation temperatures and pressures are summarized below:

		Btu/Lb		
Sat T_2, deg. F	Sat P_2, psia	h_2^{SL}	H_2^{SV}	x_2
230	20.78	198.32	1157.1	0.0343
220	17.19	188.22	1153.5	0.0445
200	11.53	168.07	1145.9	0.0645
100	0.95	68.05	1105.0	0.1573

The above numerical results are plotted on Figure 10 as valve exit temperature versus exit pressure and on Figure 11 as stream quality (wt. % vapor) versus exit P, both over the pressure range of 1000 psia down to about 10 psia.

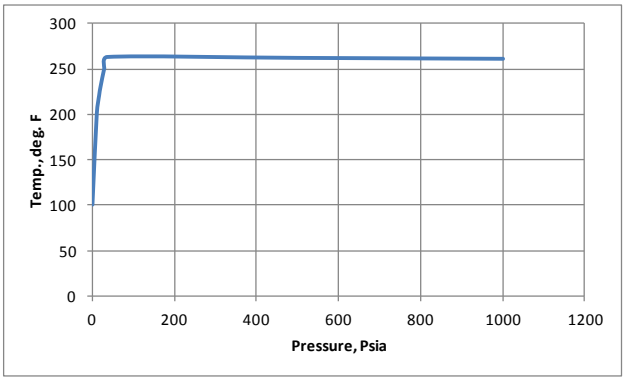

Figure 10. Effect of Isenthalpic Throttling of Compressed Liquid Water

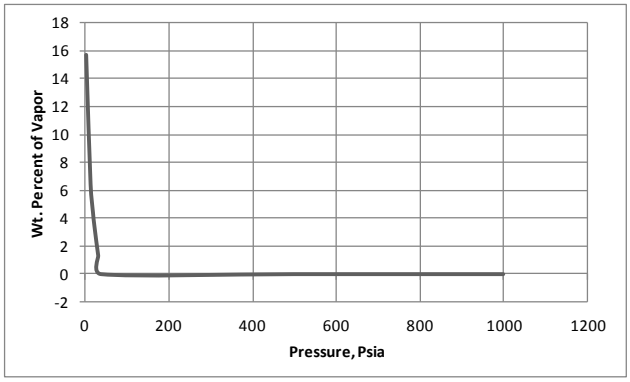

Figure 11. Steam Quality Versus Pressure

The Throttling Calorimeter The throttling calorimeter, which is frequently used to determine the quality of steam in a "wet" pipeline, is basically a constant enthalpy device. A typical throttling calorimeter setup used in conjunction with a steam pipeline is illustrated below:

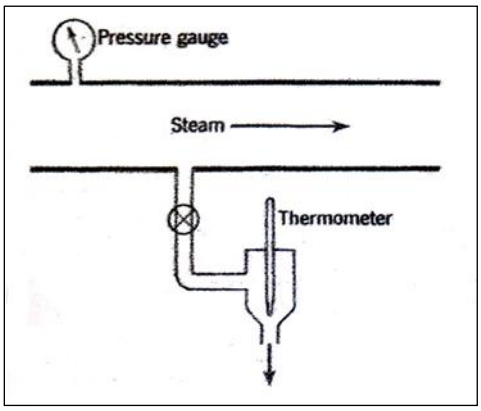

Diagram 1. Throttling Calorimeter

Steam is bled from the main line through an expansion valve into a small cylinder open to the atmosphere. By knowing the temperature of the steam in the cylinder (superheated at atmospheric pressure) and the pressure in the main line, the quality of the steam in the line may be evaluated by following a constant-enthalpy path from the final state back to the line pressure. In essence, we would be using Equation 7 in the reverse manner. For this process the heat balance equation yields the following expression for the steam quality in the line:

$$x = \frac{H_T - h_L}{\Delta H_{vap}} \qquad (23)$$

where x = weight fraction of vapor (steam quality)

H_T = total steam enthalpy obtained from the calorimeter conditions

h_L = saturated liquid enthalpy at the line pressure

ΔH_{vap} = latent heat of vaporization at the line pressure

Illustration 5 A throttling calorimeter attached to a steam line reads 220 deg. F (superheated at atmospheric pressure). The line pressure itself is 20 psig. What is the steam quality in the pipeline?

The following enthalpies were read from the steam tables of Keenan, Keyes (6):

At the calorimeter conditions of T = 220 deg. F and P = 14.7 psia

H_T = 1154.4 Btu/Lb

In the main line for saturated (wet) steam:

P = 20 + 14.7 = 34.7 psia (T_{sat} = 259 deg. F)

h_L = 228.0 Btu/Lb ; ΔH_{vap} = 939.3 Btu/Lb

Then from Equation 23 we calculate,

$$x = \frac{1154.4 - 228.0}{939.3} = 0.986 \; wt. \; fraction \; vapor$$

This basically means that 1.4 wt. % of the "wet" steam in the line is liquid water.

II. Nature and Measurement of the Joule-Thomson Coefficient

Introduction At this point we wish to focus once again on the nature and measurement of the Joule-Thomson coefficient. The sign and magnitude of μ_{JT} determines whether a fluid cools or warms when subjected to an isenthalpic expansion and the extent of the resulting temperature change.

The Joule Experiment In 1843 James Prescott Joule (7) performed a preliminary experiment which eventually led to the discovery of the Joule-Thomson isenthalpic flow effect. The apparatus he employed is described below:

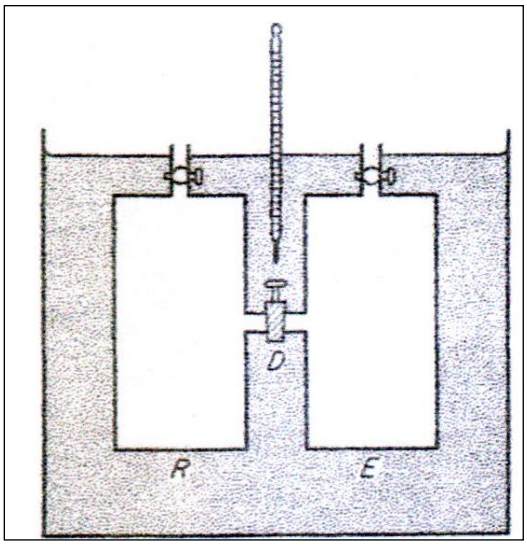

Diagram 2. The Joules Apparatus.

Joule described his experiment as follows:

> "I provided another copper receiver (E) which had a capacity of 134 cubic inches ... I had a piece D attached, in the center of which there was a bore 1/8 inch in diameter, which could be closed perfectly by means of a proper stopcock..... Having filled the receiver R with about 22 atmospheres of dry air and having exhausted the receiver E by means of an air pump, I screwed them together and put them into a tin can containing 16 1/2 lb. of water. The water was first thoroughly stirred, and its temperature taken by the same delicate thermometer which was made use of in the former experiments on mechanical equivalent of heat. The stopcock was then opened by means of a proper key, and the air allowed to pass from the full into the empty receiver until equilibrium was established between the two. Lastly, the water was again stirred and the temperature carefully noted."

Following this experimental work, Joule presented a table of experimental data, showing that there was no measurable temperature change, and arrived at the conclusion that "no change of temperature occurs when air is allowed to expand in such a manner as not to develop mechanical power i.e. so as to do no external work.

The expansion described by Joule above, with air rushing from R into the evacuated vessel E, is a typical irreversible process. Inequalities of temperature and pressure arise throughout the system, but eventually a state of equilibrium is reached. Application of the First Law here indicates no change in the internal energy of the gas since no work was done by or on it, and no heat has been exchanged with the surrounding water bath - otherwise the temperature of the water would have changed. Therefore dE = 0, and experimentally it was observed that dT = 0. It would logically then be concluded that the internal energy must depend only on temperature and not on volume. Mathematically, this conclusion can be expressed as follows:

$$dE = \left(\frac{\partial E}{\partial V}\right)_T dV + \left(\frac{\partial E}{\partial T}\right)_V dT = 0$$

or

$$\left(\frac{\partial E}{\partial V}\right)_T = -C_v \left(\frac{\partial T}{\partial V}\right)_E$$

Then

$$\left(\frac{\partial E}{\partial V}\right)_T must = 0 \quad if \quad \left(\frac{\partial T}{\partial V}\right)_E = 0$$

The fallacy here is that Joule's experiment was not capable of detecting small effects since the heat capacity of his water calorimeter (bath) was extremely large compared to that of the gas used.

The Joule-Thomson Experiment William Thomson (Lord Kelvin) suggested a much better procedure than the Joule experiment. Working with Joule, he carried out a series of experiments between 1852 and 1862 employing the apparatus represented schematically below:

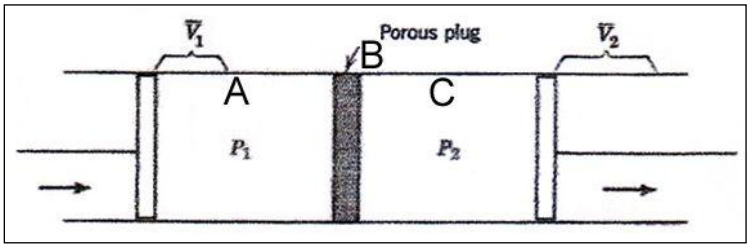

Diagram 3. The Joule-Thompson Apparatus.

The principle involves the throttling of the gas flow from a high pressure side A to a low pressure side C by interposing a porous plug B. The pressure on the A-side is maintained constant at P_1, and that on the C-side is maintained constant at a lower value P_2. This is made possible by the action of the two pistons shown. The effect of the porous plug is to allow the gas to pass slowly from A into C and thus promotes equilibrium. As a result, the temperature can be measured directly and with a high degree of accuracy. The entire system is thermally insulated, so that the process is an adiabatic one i.e. q = 0.

The volume at the left (side A) decreases by V_1 per mole of gas passing through the plug, and the volume on the right (side C) increases by V_2 per mole. As a result, the work done on the gas by the piston at the left is P_1V_1, and the work done by the gas on the piston on the right is P_2V_2. Therefore, the First Law for this case may be written as,

$$E_2 - E_1 = -w = -\left(P_2 V_2 - P_1 V_1\right) \qquad (24)$$

or

$$E_2 + P_2 V_2 = E_1 + P_1 V_1 \qquad (25)$$

$$H_2 = H_1 \qquad (26)$$

Thus the enthalpy of the gas does not change in the expansion process. The numerical value of the slope of an isenthalpic curve on a T-P diagram at any point condition is called the Joule-Thomson or the Joule-Kelvin coefficient and is denoted by the symbol μ_{JT}. Thus,

$$\mu_{JT} = \left(\frac{\partial T}{\partial P}\right)_H \qquad (27)$$

In the system or JT experiment described above Equation 27 effectively defines the temperature change per atmosphere difference in pressure measured at constant enthalpy.

With most gases with the exception of hydrogen and helium a cooling effect is obtained at room temperature because the Joule-Thomson coefficient is positive. For hydrogen at room temperature, the JT coefficient is negative. However, for hydrogen, there exists an inversion temperature at around - 78 deg. C (where $\mu_{JT} = 0$) below which the JT coefficient is positive and hydrogen is cooled by the expansion. The inversion temperature of a gas is highly dependent upon the pressure. The JT effect has very important industrial applications such as in the liquefaction of air and other gases.

The JT Inversion Curve The figure shown below shows a whole series of isenthalpic curves and the inversion curve plotted on a temperature versus pressure diagram, specifically for nitrogen (8).

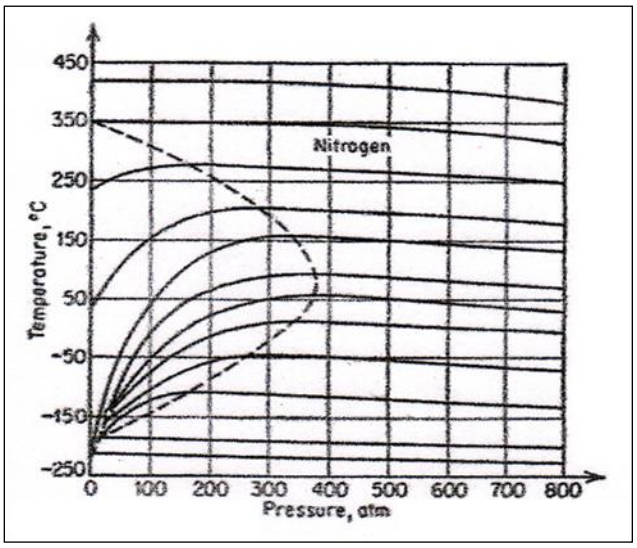

Figure 12. Isenthalpic / Inversion Curves for Nitrogen.

The series of individual plots at conditions of constant enthalpy are represented as solid curves. The locus of all points at which the JT coefficient is zero i.e. the locus of the maxima of the isenthalpic curves, is known as the inversion curve and is shown as a dotted closed curve. The region inside the inversion curve where $\mu_{JT,}$ as defined by Equation 27, is positive is called the region of cooling, whereas outside of the dotted locus, where μ_{JT} is negative, is the region of heating.

If a vertical line is drawn at an arbitrary pressure, it will intersect the isenthalpic curves at a number of points at which μ_{JT} may be obtained by measuring the slopes of the isenthalpics at these points. At this specific pressure we then would have a set of values of μ_{JT} established at a series of different temperatures. This process can obviously then be repeated at other designated pressures.

Thermodynamic Relationships Involving μ_{JT} In order to be able to predict or calculate Joule-Thomson coefficients, we generally need to relate it to the PVT properties of the fluid of interest. Here we provide a derivation of the pertinent required general thermodynamic relationships based on the First and Second Laws.

For a closed thermodynamic system of constant composition, which exchanges only heat and work with its surroundings, there are two independent degrees of freedom. As a result, a given thermodynamic property can be related directly to two other known intensive state variables or properties.

Based on the First and Second laws of thermodynamics we can readily derive the four differential equations which relate the state properties internal energy E, enthalpy H, Helmholtz free energy A and the Gibbs free energy F to the appropriate pairs of independent variables. These equations are summarized below and apply to closed systems only:

$$d\,E = T\,dS - P\,dV \qquad (28)$$

and since $H = E + PV$

then $d\,H = T\,dS + V\,dP \qquad (29)$

Next, by definition $A = E - TS$

therefore $d\,A = -S\,dT - P\,dV \qquad (30)$

Also by definition $F = H - TS = A + PV$

and finally $d\,F = -S\,dT + V\,dP \qquad (31)$

The four Maxwell equations for closed systems are readily derived from Equations 28-31 above using Green's theorem in a plane. The complete mathematical details of this theorem are not presented here but only the highlights or results of its application to exact or perfect differential equations.

First let us consider the general mathematical expression for an exact or perfect differential dZ in terms of two independent variables x and y:

$$dZ = M\,dx + N\,dy \qquad (32)$$

When the dependent variable Z is integrated over an entire process cycle or region, we get,

$$\int_c d\,Z = 0 \qquad (33)$$

Another very important mathematical characteristic of a perfect differential is that,

$$\left(\frac{\partial M}{\partial y}\right)_x = \left(\frac{\partial N}{\partial x}\right)_y \qquad (34)$$

If this latter condition is applied specifically to Equation 28, the result is,

$$\left(\frac{\partial T}{\partial V}\right)_S = -\left(\frac{\partial P}{\partial S}\right)_V \qquad (35)$$

Equation 35 is commonly referred to as the first Maxwell equation. In a similar fashion Equation 34 can be applied to the three remaining differential equations 29, 30 and 31. All four Maxwell equations for closed thermodynamic systems involving PV work only are summarized below:

Differential Eqn.	*Maxwell Eqn.*
$dE = T\,dS - P\,dV$	$\left(\frac{\partial T}{\partial V}\right)_S = -\left(\frac{\partial P}{\partial S}\right)_V$
$d\,H = T\,dS + V\,dP$	$\left(\frac{\partial T}{\partial P}\right)_S = \left(\frac{\partial V}{\partial S}\right)_P$
$d\,A = -S\,dT - P\,dV$	$\left(\frac{\partial S}{\partial V}\right)_T = \left(\frac{\partial P}{\partial T}\right)_V$
$d\,F = -S\,dT + V\,dP$	$\left(\frac{\partial S}{\partial P}\right)_T = -\left(\frac{\partial V}{\partial T}\right)_P$

Next we need to consider two very important rigorous relationships which give the isothermal effect of volume on the internal energy and the isothermal effect of pressure on enthalpy. If we take Equation 28 and differentiate it throughout with respect to volume at constant temperature, the result is,

$$\left(\frac{\partial E}{\partial V}\right)_T = T\left(\frac{\partial S}{\partial V}\right)_T - P \qquad (36)$$

If we substitute the third Maxwell equation listed above into Equation 36, the result becomes the first thermodynamic equation of state.

$$\left(\frac{\partial E}{\partial V}\right)_T = T\left(\frac{\partial P}{\partial T}\right)_V - P \qquad (37)$$

Next a similar derivation is performed starting with Equation 29. In this case we differentiate Equation 29 throughout with respect to pressure at fixed temperature.

$$\left(\frac{\partial H}{\partial P}\right)_T = T\left(\frac{\partial S}{\partial P}\right)_T + V \qquad (38)$$

Then the fourth Maxwell relation is substituted into the above expression to yield the second thermodynamic equation of state.

$$\left(\frac{\partial H}{\partial P}\right)_T = V - T\left(\frac{\partial V}{\partial T}\right)_P \qquad (39)$$

It is important to note here that the right hand sides of both Equations 37 and 39 are exclusively functions of the properties P, V and T. This makes evaluation by an equation of state quite convenient.

Let us consider the enthalpy to be a function of the two independent variables P and T. And, since enthalpy H is a state thermodynamic property, we can write the exact differential expansion for H in terms of P and T as follows,

$$d\,H = \left(\frac{\partial H}{\partial T}\right)_P d\,T + \left(\frac{\partial H}{\partial P}\right)_T d\,P \qquad (40)$$

By definition the temperature derivative in Equation 40 is the isobaric heat capacity C_P.

Therefore

$$d\,H = C_P\,d\,T + \left(\frac{\partial H}{\partial P}\right)_T d\,P \qquad (41)$$

For an isenthalpic expansion, dH = 0, and Equation 41 can be rearranged and then solved explicitly for the Joule-Thomson coefficient,

$$0 = C_P\,dT + \left(\frac{\partial H}{\partial P}\right)_T dP$$

and then

$$\left(\frac{\partial T}{\partial P}\right)_H = -\frac{1}{C_P}\left(\frac{\partial H}{\partial P}\right)_T \qquad (42)$$

where obviously $\mu_{JT} = (\partial T/\partial P)_H$, the Joule-Thomson coefficient.

Now if we substitute the second thermodynamic equation of state (Eqn. 39) into Equation 42, we arrive at the final desired expression for the JT coefficient expressed in terms of PVT properties and the isobaric heat capacity.

$$\mu_{JT} = \left(\frac{\partial T}{\partial P}\right)_H = -\frac{1}{C_P}\left[V - T\left(\frac{\partial V}{\partial T}\right)_P\right] \qquad (43)$$

Most closed equations of state, such as the Soave equation, are expressed as explicit functions of the molar volume i.e. P = f(V,T), and the volumetric derivative above is quite inconvenient to evaluate. Therefore this derivative must be transformed to an equivalent or more convenient form using the chain rule of partial differentiation.

For a function of the form f(P,V,T) = 0, where two of the variables are independent and one dependent, the chain rule can be expressed as,

$$\left(\frac{\partial P}{\partial V}\right)_T \left(\frac{\partial V}{\partial T}\right)_P \left(\frac{\partial T}{\partial P}\right)_V = -1$$

Solving for $\left(\frac{\partial V}{\partial T}\right)_P$:

$$\left(\frac{\partial V}{\partial T}\right)_P = -\frac{\left(\frac{\partial P}{\partial T}\right)_V}{\left(\frac{\partial P}{\partial V}\right)_T}$$

This latter identity is readily substituted into Equation 43 to give,

$$\mu_{JT} = \left(\frac{\partial T}{\partial P}\right)_H = -\frac{1}{C_P}\left[V + T\frac{\left(\frac{\partial P}{\partial T}\right)_V}{\left(\frac{\partial P}{\partial V}\right)_T}\right] \qquad (44)$$

Both of the pressure derivatives can be calculated from the appropriate equation of state of the form P = f(V,T). The remaining property which needs to be evaluated here is the isobaric heat capacity, C_P. Then we will have all of the terms or properties required to evaluate Equation 44 for μ_{JT}.

First we consider the internal energy E to be a function of the two independent variables T and V and then write the exact differential expansion for E as,

$$dE = \left(\frac{\partial E}{\partial T}\right)_V dT + \left(\frac{\partial E}{\partial V}\right)_T dV \qquad (45)$$

By definition, the temperature derivative above is known as the isochoric or constant volume heat capacity, C_V. Therefore,

$$dE = C_V\, dT + \left(\frac{\partial E}{\partial V}\right)_T dV \qquad (46)$$

Then we substitute Equation 37 into Equation 46 to get,

$$dE = C_V\, dT + \left[T\left(\frac{\partial P}{\partial T}\right)_V - P\right] dV \qquad (47)$$

If Equation 34 (Maxwell Equation) is applied to the exact differential expression above, the result becomes,

$$\left(\frac{\partial C_V}{\partial V}\right)_T = \frac{\partial\left[T\left(\frac{\partial P}{\partial T}\right)_V - P\right]_V}{\partial T} = T\left(\frac{\partial^2 P}{\partial T^2}\right)_V$$

This expression can readily be integrated between the limits of the ideal gas state and the real fluid state to give the real fluid isochoric heat capacity relative to the ideal gas value at the same temperature.

$$C_V - C_V^o = T\int_{\infty}^{V}\left(\frac{\partial^2 P}{\partial T^2}\right)_V dV \qquad (48)$$

Without providing a detailed derivation, we simply provide the expression relating the real fluid isobaric and isochoric heat capacities below,

$$C_P - C_V = T\left(\frac{\partial P}{\partial T}\right)_V\left(\frac{\partial V}{\partial T}\right)_P \qquad (49)$$

Using the chain rule as applied previously, we can readily substitute for the volume derivative shown in Equation 49 to yield Equation 50,

$$C_P - C_V = -T\frac{\left(\frac{\partial P}{\partial T}\right)_V^2}{\left(\frac{\partial P}{\partial V}\right)_T} \qquad (50)$$

Once C_V is computed from Equation 48, C_P is then readily computed directly from Equation 50. The ideal gas isochoric heat capacity is simply determined from the ideal gas isobaric capacity via the relation,

$$C_V^o = C_P^o - R \qquad (51)$$

C_P^o is computed at system temperature from Equation 15 and the appropriate coefficients read from Table 1. Thus, in order to compute JT coefficients from a volume explicit closed equation of state (P = f(V,T)), the following pressure derivative functions need to be evaluated:

$$\left(\frac{\partial P}{\partial T}\right)_V \quad ; \quad \left(\frac{\partial^2 P}{\partial T^2}\right)_V \quad ; \quad \left(\frac{\partial P}{\partial V}\right)_T$$

In Section IV the appropriate expressions for these derivatives will be derived for several cubic-in-volume closed equations of state. Then, JT coefficients can be predicted from these equations of state and subsequently compared with the corresponding measured coefficients.

Illustration 6 A gas at 100 deg. F, with a fixed C_P value of 7.0 Btu/Lbmole-^oR, has a Joule-Thomson coefficient that obeys the relation,

$$\mu_{JT} = 0.0032 - 0.0008P$$

where P is in units of atmospheres and μ_{JT} is expressed in units of deg. R/atm. For this particular gas let us calculate and plot as a function of pressure over the range 0 to 20 atm, the following:

1. the JT coefficient itself at 100 deg. F

2. the enthalpy relative to zero pressure, H - H^o, in Btu/Lbmole

At what pressure does the JT inversion point occur ?

First we need to derive the appropriate expression for the enthalpy departure for this gas at 100 deg. F. This can readily be done by substituting the above pressure-dependent function for μ_{JT} into Equation 42, Thus,

$$\mu_{JT} = -\frac{1}{C_P}\left(\frac{\partial H}{\partial P}\right)_T = 0.0032 - 0.0008P,\ \text{deg}.R/Atm$$

Upon integration of this equation between the limits of an ideal (P = 0) and the real gas state at P, we get,

$$\int_{H^o}^{H} dH = -C_P \int_0^P (0.0032 - 0.0008P)\,dP$$

$$H - H^o = -C_P \left[0.0032P - 0.0004P^2\right]_0^P$$

$$= -C_P \left[0.0032P - 0.0004P^2\right]$$

If C_P is expressed in units of Btu/Lbmole-deg. R, then the enthalpy departure above will turn out to be in units of Btu/Lbmole. Figure 13 and Figure 14 show the JT coefficient and enthalpy departure respectively plotted versus pressure up to 20 atmospheres.

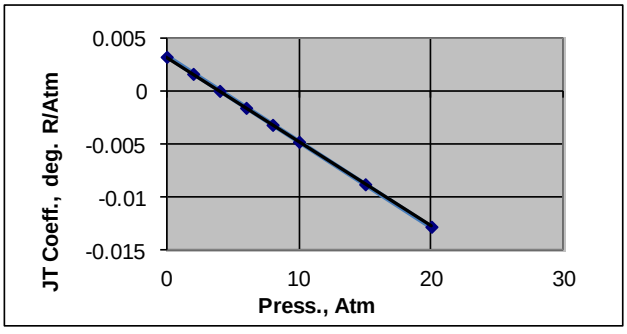

Figure 13. JT Coeff. Versus Pressure.

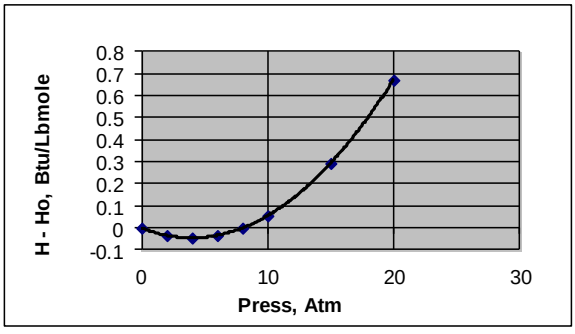

Figure 14. Enthalpy Departure vs. Pressure.

The inversion pressure where $\mu_{JT} = 0$ occurs at a value of 4 atm. Also at this point, the enthalpy of the system reaches a minimum value or $H - H^o = -0.0448$ Btu/Lbmole. At P = 8 atm, the enthalpy departure from the ideal gas state returns to zero. And above 8 atm, the departure becomes positive i.e. the real gas enthalpy exceeds that of the ideal gas value.

Illustration 7 In his textbook entitled "Chemical and Engineering Thermodynamics", Sandler (9) extracted some second virial coefficient data for nitrogen from the classical work of Dymond and Smith (10). Sandler's tabulation is shown below and provides the second virial coefficient as a function of temperature from 75 to 700 deg. K.

Temp. (^{o}K)	B (cc/gmole)
75	- 274
100	- 160
125	- 104
150	- 71.5
200	- 35.2
250	- 16.2
300	- 4.2
400	+ 9.0
500	+ 16.9
600	+ 21.3
700	+ 24.0

From both experimental studies and statistical mechanics it is well known that at moderate pressures, the volumetric behavior of gases obey the open virial equation of state truncated after the second virial coefficient, B. Here B is exclusively a function of temperature only. Using the virial equation written as PV = RT + BP, where V is the molar volume, we are asked to determine (estimate) the Boyle temperature (the temperature at which B = 0) and the inversion temperature(s) for gaseous nitrogen from the above tabulation of B-values for nitrogen.

First we solve the truncated virial equation above for V and substitute the result directly into Equation 43 to get the appropriate expression for μ_{JT}.

$$V = \frac{RT}{P} + B \quad ; \quad \left(\frac{\partial V}{\partial T}\right)_P = \frac{R}{P} + \frac{dB}{dT}$$

and therefore

$$\mu_{JT} = -\frac{1}{C_P}\left[V - T\left(\frac{\partial V}{\partial T}\right)_P\right] = -\frac{1}{C_P}\left[\frac{RT}{P} + B - \frac{RT}{P} - T\frac{dB}{dT}\right]$$

$$\mu_{JT} = -\frac{1}{C_P}\left[B - T\frac{dB}{dT}\right]$$

The above expression requires that we calculate the first temperature derivative of the second virial coefficient from the basic data shown graphically as B vs.T in Figure 15. As a result, it would be quite convenient to have a relatively simple analytic representation of the data. A successful least-squares fit was achieved using a hyperbolic function of the form,

$$B = \frac{A + B' T}{1 + C T} \qquad (52)$$

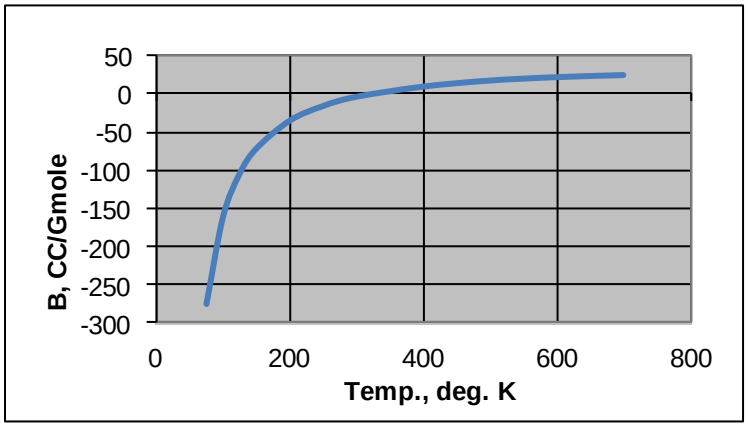

Figure 15. Second Virial Coefficient for Nitrogen.

The following regression constants were obtained for the 11 data points listed above by Sandler.

$$A = 413.4512 \quad ; \quad B' = -1.253687 \quad ;$$

$$C = -0.02837002$$

The overall absolute average deviation and standard deviation produced by Equation 52 turn out to be 4.1 and 6.6 percent respectively.

The Boyle temperature is defined by the exact mathematical limit:

$$Lim(V \to \infty)\left[V\left(\frac{PV}{RT} - 1 \right) \right] = Lim\left(V \to \infty\right) B = 0$$

If we apply this constraint to Equation 52, then,

$$A + B' T = 0$$

or

$$T_B = -\frac{A}{B'} = -\frac{413.4512}{-1.253687} = 329.8 \text{ deg}.K$$

which is an estimate of the Boyle temperature consistent with the virial coefficient data provided us.

At any inversion point, the JT coefficient assumes a value of zero. Therefore, we have,

$$\mu_{JT} = -\frac{1}{C_P}\left[B - T\frac{dB}{dT}\right] = 0 \;\; or \;\; B = T\frac{dB}{dT}$$

As a result, we need to differentiate Equation 52 to get dB/dT.

$$\frac{dB}{dT} = \frac{B'}{1+CT} - \frac{C\left(A+B'T\right)}{\left(1+CT\right)^2}$$

$$\frac{dB}{dT} = \frac{B' + B'CT - AC - B'CT}{\left(1+CT\right)^2} = \frac{B' - AC}{\left(1+CT\right)^2}$$

So then, for the JT coefficient to be zero we would have,

$$\frac{A+B'T}{1+CT} = \frac{B'T - ACT}{\left(1+CT\right)^2}$$

$$\left(A+B'T\right)\left(1+CT\right) = B'T - ACT$$

This equation is readily rearranged into a form which is a quadratic in temperature, the result

$$T^2 + \frac{2A}{B'}T + \frac{A}{B'C} = 0$$

Next the numerical values of A, B$'$ and C are substituted and the resulting equation solved for T.

$$T^2 + \frac{2\left(413.4512\right)}{\left(-1.253687\right)}T + \frac{413.4512}{\left(-1.253687\right)\left(-0.02837002\right)} = 0$$

or

$$T^2 - 659.576T + 11,624.54 = 0$$

Application of the general quadratic formula here yields the final result.

$$T = \frac{659.576 \pm \sqrt{\left(659.576\right)^2 - 4\left(11,624.54\right)}}{2}$$

$$T = \frac{659.576 \pm 623.332}{2} = 641.5 \text{ deg.}K \; or \; 18.1 \text{ deg.}K$$

These values are the calculated (estimated) inversion point temperatures. The lower temperature of 18 deg. K is highly suspect because it falls outside of the temperature range of the original B versus T data.

III. Generalized JT Inversion Curve in Corresponding States Format

Introduction It is possible to generate a generalized inversion curve for fluids within the framework of the Law of Corresponding States. The simple van der Waals (VDW) equation of state is capable of predicting inversion PVT conditions for a fluid. This equation can be inserted into Equation 44 with the constraint that $\mu_{JT} = 0$, and the appropriate interrelationships between P, V and T can easily be derived and placed in a convenient corresponding states framework involving reduced coordinate parameters ($T_R = T/T_c$, $P_R = P/Pc$). Miller (11) has also developed and recommended a three-constant equation for approximating the inversion curve locus in reduced coordinate form.

Perry's Chemical Engineers' Handbook (12) tabulates approximate inversion-curve loci for several light hydrocarbons and non hydrocarbon gases. These data were reduced to a corresponding states framework and subsequently plotted and compared against the generalized inversion curves predicted by the VDW and Miller equations. In addition, we observed that the series of inversion curves for the non polar gas components appeared to follow a systematic pattern. All of these comparisons and observations are discussed in detail below.

VDW Equation as a Basis If we begin with the rigorous relationship between the JT coefficient and PVT properties, i.e. Equation 44, and impose the constraint that $\mu_{JT} = 0$, we can readily write,

$$V + T\frac{\left(\frac{\partial P}{\partial T}\right)_V}{\left(\frac{\partial P}{\partial V}\right)_T} = 0 \qquad (53)$$

From the van der Waals equation written in the form,

$$P = \frac{RT}{V-b} - \frac{a}{V^2} \qquad (54)$$

we first develop expressions for the pressure derivative functions.

$$\left(\frac{\partial P}{\partial T}\right)_V = \frac{R}{V-b} \quad ; \quad \left(\frac{\partial P}{\partial V}\right)_T = -\frac{RT}{(V-b)^2} + \frac{2a}{V^3}$$

These derivatives are now substituted directly into Equation 53 to yield,

$$V + T\frac{\dfrac{R}{V-b}}{\dfrac{2a}{V^3} - \dfrac{RT}{(V-b)^2}} = 0$$

or

$$\frac{2a}{V^2} - \frac{V\,RT}{(V-b)^2} + \frac{RT}{V-b} = 0$$

$$RT\left[\frac{V}{(V-b)^2} - \frac{1}{V-b}\right] = \frac{2a}{V^2}$$

$$RT_{inv} = \frac{2a(V-b)^2}{V^3 - V^2(V-b)} = \frac{2a(V-b)^2}{V^2 b} \quad (55)$$

Next we take advantage of the fact that the critical constants for a van der Waals fluid can be related to the constants a and b by using the critical point criteria that,

$$\left(\frac{\partial P}{\partial V}\right)_{T_C} = \left(\frac{\partial^2 P}{\partial V^2}\right)_{T_C} = 0$$

The resulting expressions for the critical volume and temperature become,

$$V_C = 3b \quad ; \quad T_C = \frac{8a}{27bR} \qquad (56a,b)$$

However, the reduced volume and temperature are related to the operating volume and temperature by the basic definitions:

$$V_R = V/V_C \quad \text{or} \quad V_C = V/V_R$$

and

$$T_R = T/T_C \quad \text{or} \quad T_C = T/T_R$$

These two expressions for V_C and T_C are then substituted directly into Equations 56 a and b to give,

$$V = 3bV_R \quad ; \quad T = \frac{8a}{27bR}T_R \qquad (57\,a,b)$$

Insertion of Equations 57 a and b into Equation 55 leads finally to the relationship between the reduced inversion temperature and the reduced volume i.e. Equation 58,

$$R\frac{8a}{27bR}T_{RInv} = \frac{2a\left(3bV_R - b\right)^2}{9b^2V_R^2 b}$$

which upon final simplification becomes,

$$T_{RInv} = \frac{3\left(3V_R - 1\right)^2}{4V_R^2} \qquad (58)$$

Now, in order to relate the inversion point to the reduced pressure a well, we need to return to the van der Waals equation itself written in the reduced coordinate form.

Starting with the van der Waals equation written as,

$$\left(P + \frac{a}{V^2}\right)\left(V - b\right) = RT$$

we need to substitute for P, V and T in terms of reduced parameters. Equations 57 a and b provide the necessary substitutions for V and T. The other relationship which relates P and P_R based on the critical point criteria described above is,

$$P_C = \frac{P}{P_R} = \frac{a}{27b^2} \qquad (59)$$

Now Equations 57 a,b and 59 are substituted directly into the van der Waals equation with the result,

$$\left[\left(\frac{a}{27b^2}\right)P_R + \frac{a}{9b^2V_R^2}\right]\left[3bV_R - b\right] = R\left(\frac{8a}{27Rb}\right)T_R$$

This expression is readily simplified as follows

$$\left[\frac{P_R}{27}+\frac{1}{9V_R^2}\right]\left[3V_R-1\right]=\frac{8}{27}T_R$$

:

$$\left[P_R+\frac{3}{V_R^2}\right]\left[3V_R-1\right]=8T_R$$

and finally,

$$\left(P_R+\frac{3}{V_R^2}\right)\left(V_R-\frac{1}{3}\right)=\frac{8}{3}T_R \qquad (60)$$

Next we substitute the expression for the inversion temperature, Eqn. 58, into the RHS of Equation 60 to get the van der Waals P_R - V_R relationship for the inversion curve.

$$\left(P_R+\frac{3}{V_R^2}\right)\left(V_R-\frac{1}{3}\right)=\frac{2\left(3V_R-1\right)^2}{V_R^2}$$

The expression is further simplified to yield a quadratic equation in V_R,

$$V_R^2-\frac{18}{P_R}V_R+\frac{9}{P_R}=0 \qquad (61)$$

Equation 61 is used in tandem with Equation 58 to generate a generalized inversion curve in corresponding states framework based on the van der Waals equation of state.

1. Set or select a value for P_R.

2. Calculate the two roots V_{R1} and V_{R2} (hopefully both real) from Eqn. 61.

3. For each value of V_R from Step 2, calculate T_{R1Inv} and T_{R2Inv} from Eqn. 58.

4. Plot both sets of T_{RInv} versus the selected value of P_R..

The numerical tabulation given below is the result of carrying out the four steps above when Equation 61 is solved using the quadratic formula i.e.

$$V_R = \frac{\frac{18}{P_R} \pm \sqrt{\left(\frac{18}{P_R}\right)^2 - \frac{36}{P_R}}}{2}$$

Eqn. 58

P_R	V_{R1}	V_{R2}	T_{R1}	T_{R2}
1	17.49	0.515	6.495	0.838
2	8.47	0.531	6.229	0.938
3	5.45	0.551	5.949	1.051
4	3.93	0.573	5.653	1.181
5	3.00	0.600	5.333	1.333
6	2.37	0.634	4.982	1.518
7	1.89	0.680	4.581	1.752
8	1.50	0.750	4.083	2.083
9	1.00	1.00	3.000	3.000

It should be noted here that inversion curve terminates at a maximum reduced pressure of 9 (T_R = 3), and only one inversion temperature exists at this point. Below P_R = 9, an upper and lower inversion temperature exists.

Miller Equation In his 1970 paper, Miller (11) utilized a host of experimental JT inversion point data for the components CO_2, N_2, CO, CH_4, NH_3. propane, Ar, and ethylene to develop a three-constant corresponding states equation. The following expression was the result of a least squares fit of the collected data:

$$P_R = 24.21 - \left(\frac{18.54}{T_R}\right) - 0.825T_R^2 \qquad (62)$$

With this correlation, a maximum inversion reduced temperature of 5.0 and a minimum inversion reduced temperature of 0.8 are produced. The maximum reduced pressure of P_R = 11.75 occurs at T_R = 2.25. Miller also concluded from his studies that none of the better simple equations of state (van der Waals, generalized Dieterici, generalized Redlich-Kwong, or Martin) adequately characterizes the inversion curve. In any case, prediction of JT inversion points is a very severe test of equations of state.

The upper and lower T_R versus P_R curves generated from the van der Waals and Miller equations have been plotted in Figure 16. The van der Waals prediction is represented by the solid curves and the predictions via the Miller equation (Eq. 62) by the dashed inversion curve. The Miller curve is generally flatter or narrower in nature than the VDW curve and displays a significantly higher maximum reduced pressure. And, in general, the VDW equation generates a significantly higher upper inversion curve than does the Miller equation.

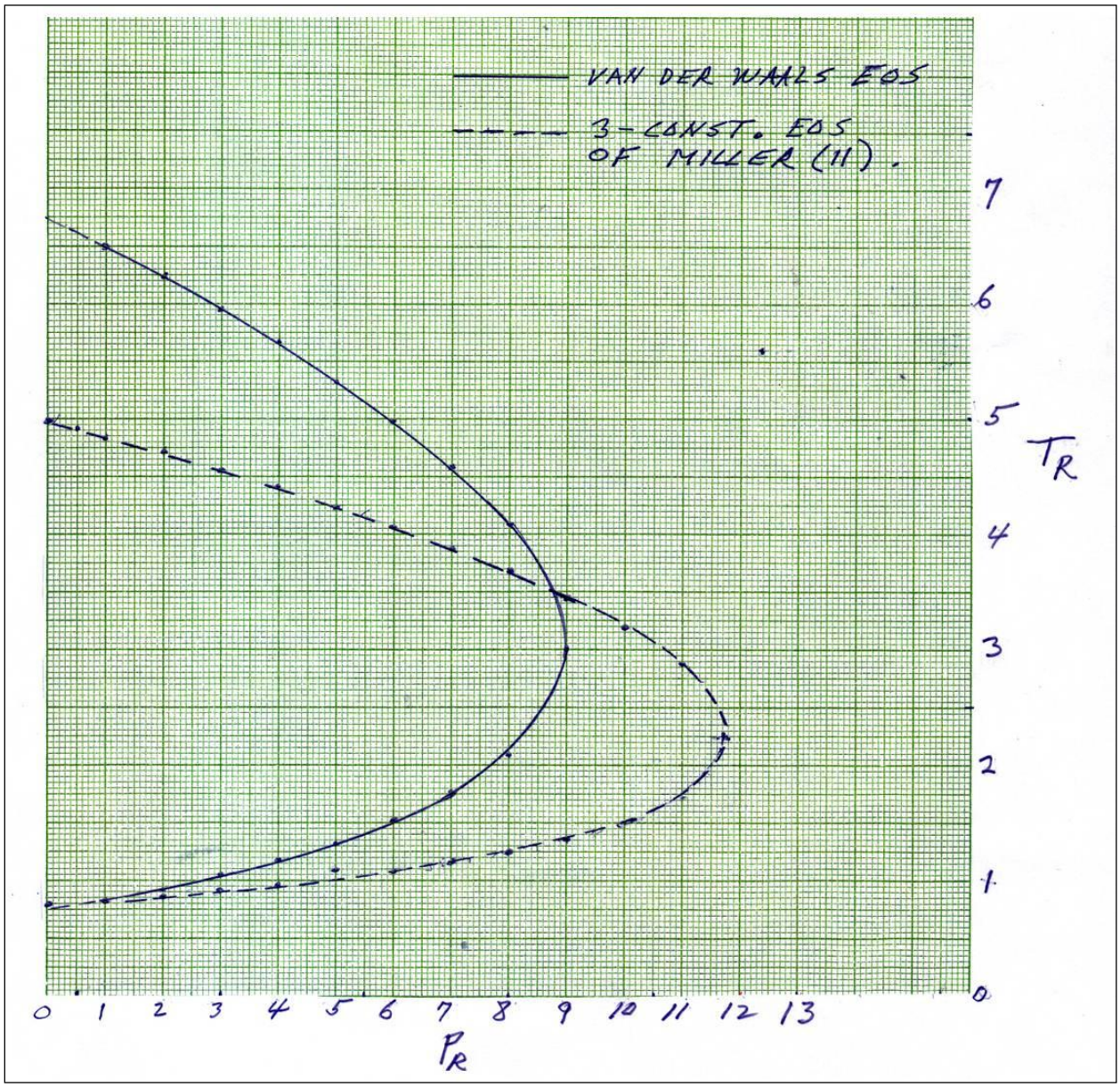

Figure 16. Generalized JT Inversion Curves Generated from the van der Waals and Miller Equations of State.

JT Inversion-Curve Loci Data Perry's Sixth Edition of the Chemical Engineers' Handbook (12) reports approximate JT inversion-curve loci (T versus P) for a host of light hydrocarbon and non hydrocarbon gases. The detailed source references for these data are listed in Table 3-149, page 3-107, of the Handbook. These data were supposedly derived from smoothed and extrapolated JT coefficients extracted from the specific data sources listed in Table 3-149. As a result, they are designated as "approximate" inversion-curve loci. Table 2 of our paper here summarizes these data. The following specific components are included:

air	normal hydrogen
argon	methane
carbon dioxide	ethane
deuterium	propane

Table 3 of our paper lists the component critical constants that were needed to transform these data to a corresponding states framework (T_R versus P_R). Both upper and lower T-P loci are reported for all components above with the exception for ethane and propane where only the lower inversion curves are reported.

On Figure 17 we have plotted all of the available upper and lower inversion points in corresponding states framework (T_R vs. P_R) for each component covered in Table 2 with the exception of deuterium. In addition, the inversion loci generated from the VDW and Miller equations are superimposed upon the data.

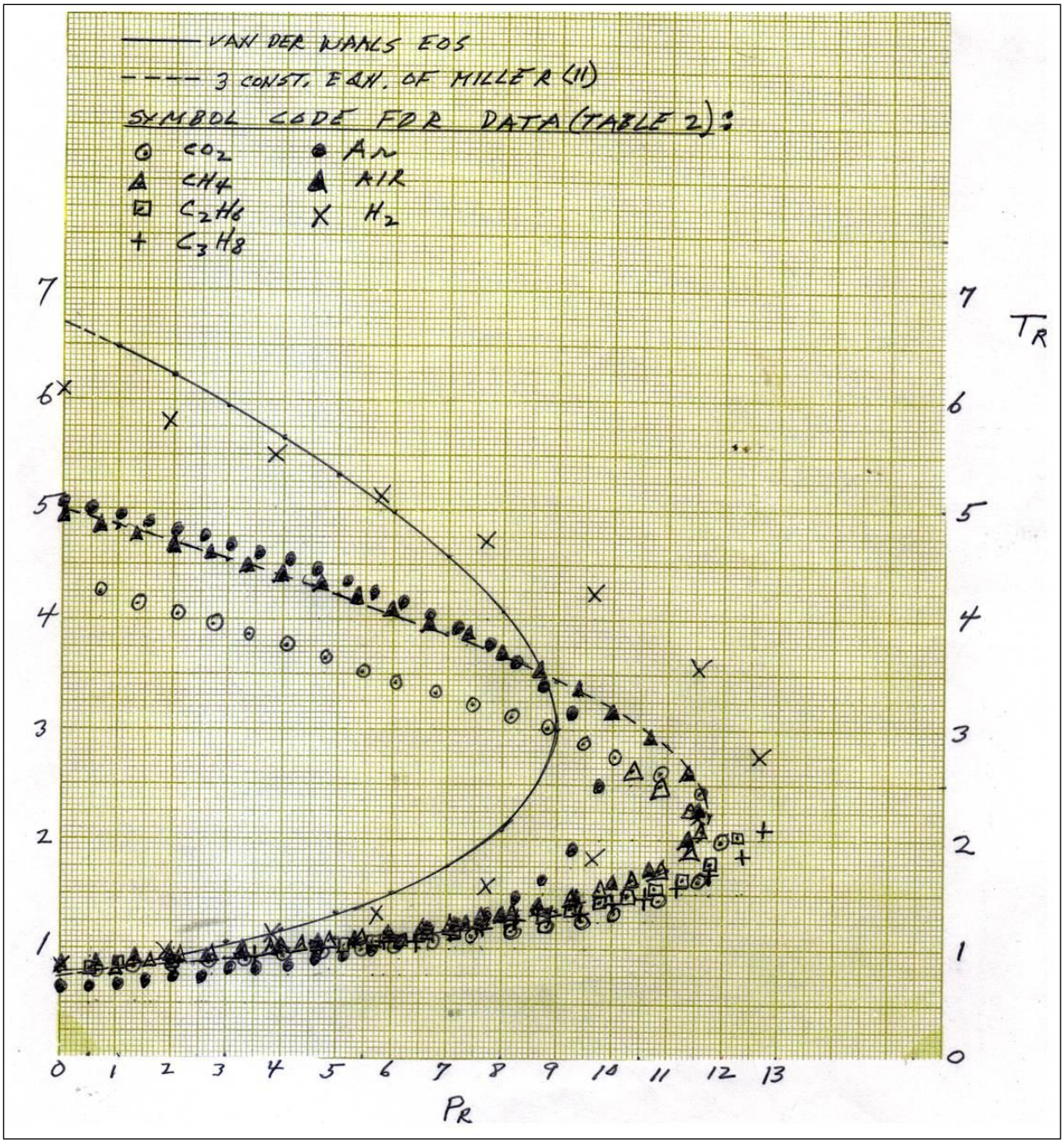

Figure 17. JT Inversion Loci for Components Listed in Table 2.

Below a reduced pressure of about 8, all of the data points, with the exception of CO_2 and H_2, fall nicely in line with one another. In this region they also follow the Miller inversion curve very closely. Above $P_R = 8$, the various component curves display more of a spread but still agree reasonably well with the Miller curve in the specific region where the reduced pressure is at a maximum. The VDW locus shows poor agreement with the data and appears to produce lower and upper inversion curves that are too high. It is not surprising that the CO_2 and H_2 loci do not fall in line with the other components since CO_2 is a polar compound, and H_2 is a quantum gas. All of the other components treated here are basically non polar compounds.

In Figure 18, we have plotted the smoothed JT inversion loci for each of the non polar gases only. As we pointed out previously, above $P_R = 8$, the various loci tend to show a spread. We classified each curve according to the value of the component's Pitzer acentric factor ω. In general, it can be observed here that the maximum P_R point increases with increasing acentric factor. The higher the acentric factor, then the higher is the departure of the molecular structure from perfect sphericity. There is probably not enough data present here to allow us to conclude that we have arrived at a generalized graphical correlation. The Miller inversion curve does, however, provide a very good overall (average) representation of the inversion loci for light non polar gases.

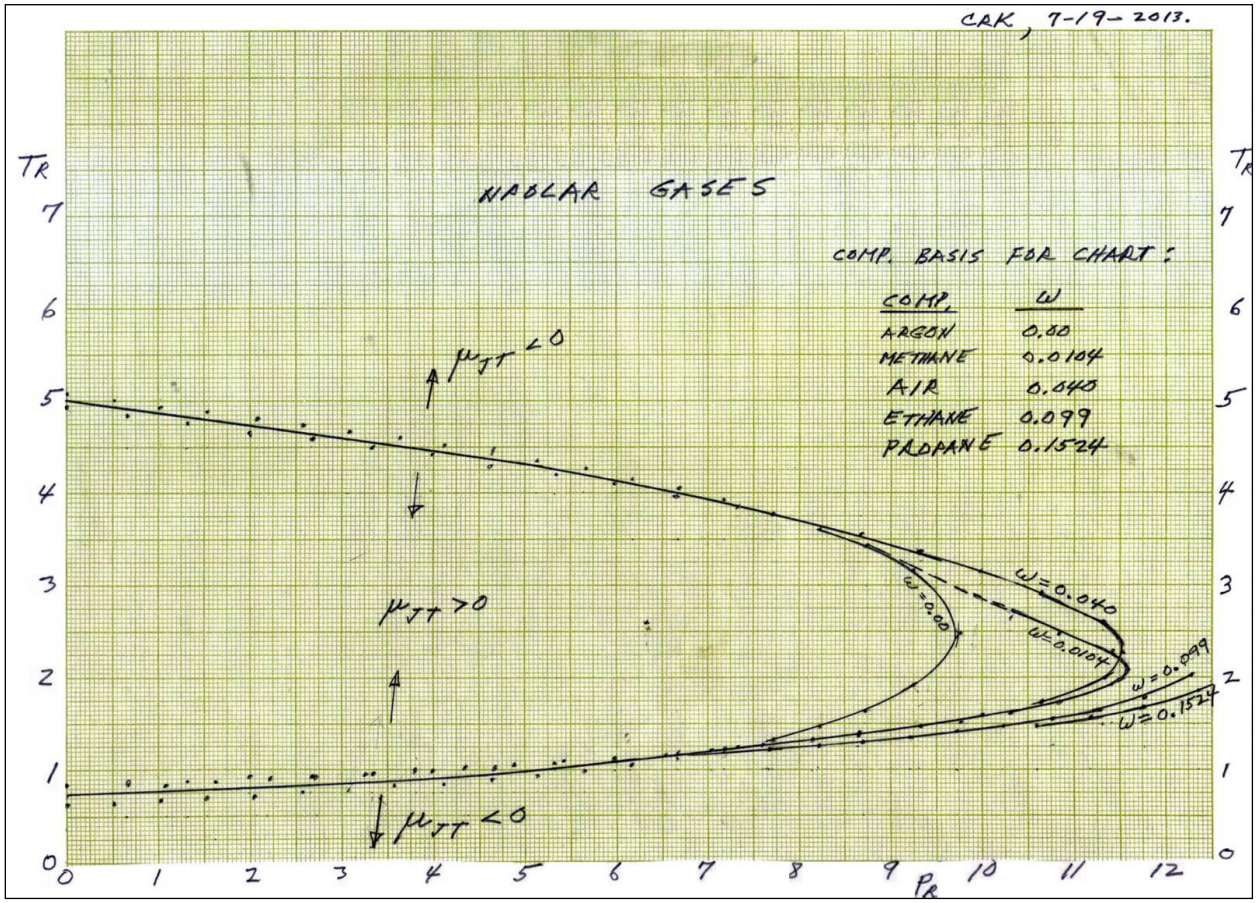

Figure 18. Generalized Corresponding States Graphical Correlation for the JT.

Finally, Figure 19 provides smoothed plots for just the individual gases H_2 and CO_2. As we discussed previously, these data do not line up with the data plotted for the non polar gases.

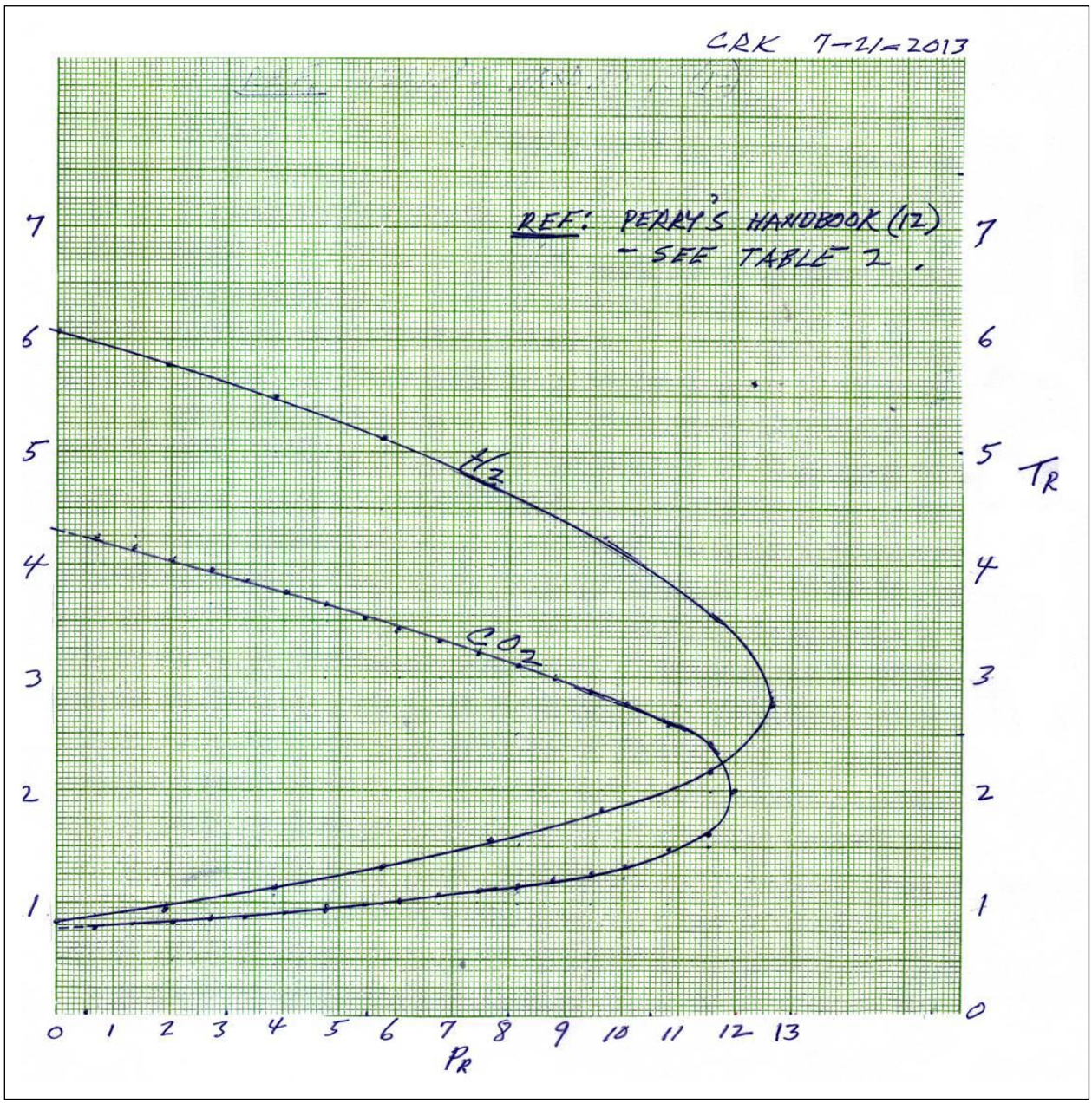

Figure 19. Smoothed Approximate JT Inversion Curves Specifically for H_2 and CO_2.

IV. Prediction of JT Coefficients from Cubic Equations of State

Experimental Data In addition to providing approximate JT inversion-curve loci data, Perry's Handbook (12) also gives measured Joule-Thomson coefficients for several non hydrocarbon gases. The specific components covered are:

air
argon
carbon dioxide
helium
nitrogen

Once again the detailed source references can be found in Table 3-149 of the Handbook. Because of time and energy constraints, we just focused our attention on the components nitrogen and carbon dioxide. We compared the measurements reported in the handbook against the corresponding predictions of the following cubic equations of state:

1. van der Waals equation
2. Redlich-Kwong equation
3. API (modified) Soave equation
4. Peng-Robinson equation

Before discussing the details of the numerical comparisons and the statistical deviations, we first briefly review the salient features of each equation of state and the relevant terms and properties that need to be calculated in order to finally predict the JT coefficient.

van der Waals Equation The first closed-cubic equation of state was proposed by the Dutch physicist J. D. van der Waals in 1873. He proposed the equation,

$$\left(P+\frac{a}{V^2}\right)(V-b)=RT \qquad (63)$$

for one mole of a single phase fluid. The term a/V^2 arises from the existence of intermolecular forces and the constant b is proportional to the volume occupied by the molecules (atoms) themselves. Equation 63 affords a most fortunate circumstance in that it can be applied to either the vapor or liquid phases. This is true because the equation is cubic in the volume, and, for a specified P and T, can have as many as three real roots for V. The largest root will generally apply to the vapor and the smallest to the liquid.

After rearrangement, Equation 63 can be transformed into a cubic polynomial in V with the result,

$$V^3-\left(b+\frac{RT}{P}\right)V^2+\left(\frac{a}{P}\right)V-\frac{ab}{P}=0 \qquad (64)$$

Equation 64 can be further transformed to a cubic in the compressibility factor after substitution of the identity V= ZRT/P with the result being,

$$Z^3-\left(\frac{bP}{RT}+1\right)Z^2+\left(\frac{aP}{R^2T^2}\right)Z-\frac{abP^2}{(RT)^3}=0 \quad (65)$$

Furthermore, we can also define the following parameters and then simplify the above expression to even a more compact form,

$$A=\frac{aP}{(RT)^2} \quad ; \quad B=\frac{bP}{RT} \qquad (66a,b)$$

After substitution of these two identities into Equation 65, the final result becomes,

$$Z^3-(B+1)Z^2+Az-AB=0 \qquad (67)$$

With this form of the VDW equation, the largest (vapor) or smallest (liquid) root will still be sought - in this case the correct value of Z. The characteristic constants a and b are simply derived from the criteria for a pure substance that both a maximum in the saturation locus and a point of inflection (on the critical isotherm) coexist at the critical point. Mathematically, these criteria are expressed as,

$$\left(\frac{\partial P}{\partial V}\right)_{T_c,P_c}=\left(\frac{\partial^2 P}{\partial V^2}\right)_{T_c,P_c}=0 \qquad (68)$$

When these criteria are applied to Equation 63, the following expressions for a and b can be derived,

$$a=\frac{27R^2T_c^2}{64P_c} \quad ; \quad b=\frac{RT_c}{8P_c} \quad ; \quad Z_c=0.375 \qquad (69a,b,c)$$

In Section II we derived the generalized thermodynamic functions required for the evaluation of the JT coefficient via a volume explicit equation of state i.e. P = f(V,T).
The key derivative terms needed were,

$$\left(\frac{\partial P}{\partial T}\right)_V \quad ; \quad \left(\frac{\partial^2 P}{\partial T^2}\right)_V \quad ; \quad \left(\frac{\partial P}{\partial V}\right)_T$$

For the van der Waals equation written in the form,

$$P=\frac{RT}{V-b}-\frac{a}{V^2} \qquad (70)$$

these derivatives become,

$$\left(\frac{\partial P}{\partial T}\right)_V = \frac{R}{V-b} \quad \left(\frac{\partial^2 P}{\partial T^2}\right)_V = 0 \quad ; \quad \left(\frac{\partial P}{\partial V}\right)_T = \frac{2a}{V^3} - \frac{RT}{(V-b)^2}$$

As a result, we readily see that Equations 48 and 50 become,

$$C_V = C_V^o$$

$$C_P - C_V = C_P - C_V^o = -T \frac{\left(\frac{R}{V-b}\right)^2}{\frac{2a}{V^3} - \frac{RT}{(V-b)^2}}$$

The ideal gas isochoric heat capacity is simply computed from the ideal gas isobaric heat capacity from the simple relation,

$$C_V^o = C_P^o - R$$

C_p^o is computed at system temperature from Equation 15 with the appropriate pure component coefficients read from Table 1. Now we have all of the terms necessary to evaluate Equation 44 for the JT coefficient.

$$\mu_{JT} = -\frac{1}{C_P}\left[V + T\frac{\left(\frac{R}{V-b}\right)}{\left(\frac{2a}{V^3} - \frac{RT}{(V-b)^2}\right)}\right] \qquad (71)$$

Needless to say, we need to use a consistent set of units for each term in Equation 71 in order to calculate the JT coefficient in the desired system of units (deg. R/psia, deg. K/atm, etc.).

Redlich-Kwong Equation Many extensions of the van der Waals equation have been proposed and published. One of the first modifications of any significance was the Redlich-Kwong equation (13). The proposed equation is written as,

$$P=\frac{RT}{V-b}-\frac{a}{T^{0.5}V\left(V+b\right)} \qquad (72)$$

where a and b are true constants characteristic of the particular fluid of interest. The authors have transformed this equation to the compressibility factor form after substitution the following identities:

$$A^2=\frac{a}{R^2T^{2.5}} \quad ; \quad B=\frac{b}{RT}$$

$$h=\frac{BP}{Z} \quad ; \quad V=\frac{ZRT}{P}$$

The result is,

$$Z=\frac{1}{1-h}-\frac{\left(A^2/B\right)h}{1+h} \qquad (73)$$

Once again, the correct root (V or Z) for either the vapor or liquid must be determined by an iterative procedure. Like the VDW equation, the RK constants can also be related directly to the critical constants by applying Equation 68 to Equation 72.

$$a=\frac{0.4278R^2\ T_c^{2.5}}{P_c} \quad ; \quad b=\frac{0.0867RT_c}{P_c} \qquad (74a,b)$$

For the evaluation of the JT coefficient using the RK equation, the following quantities need to be substituted into Equation 44:

$$\left(\frac{\partial P}{\partial T}\right)_V=\frac{R}{V-b}+\frac{0.5a}{T^{1.5}V\left(V+b\right)} \quad ; \quad \left(\frac{\partial^2 P}{\partial T^2}\right)_V=-\frac{0.75a}{T^{2.5}V\left(V+b\right)}$$

$$\left(\frac{\partial P}{\partial V}\right)_T=-\frac{RT}{\left(V-b\right)^2}+\frac{a\left(2V+b\right)}{T^{0.5}\left[V\left(V+b\right)\right]^2}$$

From Equation 48 we have,

$$C_V-C_V^o=-\frac{0.75a}{T^{2.5}}T\int_{\infty}^{V}\frac{dV}{V\left(V+b\right)}=-\frac{0.75a}{bT^{1.5}}Ln\left(\frac{V}{V+b}\right) \quad ; \quad C_V^o=C_P^o-R$$

and from Equation 50,

$$C_P - C_V = -T \frac{\left[\frac{R}{V-b} + \frac{0.5a}{T^{1.5}V(V+b)}\right]^2}{\left[\frac{a}{T^{0.5}}\frac{2V+b}{\left(V(V+b)\right)^2} - \frac{RT}{(V-b)^2}\right]}$$

And finally, the appropriate expressions above can be substituted into Equation 44 for the prediction of the JT coefficient via the RK equation of state.

Soave Equation In 1971 G. Soave (14) proposed what is probably the most popular and extensively used cubic equation of state. Basically, Soave modified the RK equation by replacing the term $a/T^{0.5}$ with a more generalized temperature-dependent term a(T). Thus,

$$P = \frac{RT}{V-b} - \frac{a(T)}{V(V+b)} \qquad (75)$$

The Z-form of the Soave equation is derived by making the following substitutions:

$$V = \frac{ZRT}{P} \quad ; \quad A = \frac{aP}{R^2T^2} \quad ; \quad B = \frac{bP}{RT} \qquad (76a,b,c)$$

with the result being,

$$Z^3 - Z^2 + Z\left(A - B - B^2\right) - AB = 0 \qquad (77)$$

Specifically for the Soave equation,

$$a(T_C) = a_C = \frac{0.42747\,R^2T_C^2}{P_C} \qquad (78)$$

$$b = \frac{0.08664\,RT_C}{P_C} \quad ; \quad Z_C = 0.333 \qquad (79a,b)$$

The key feature of the Soave approach here is the comprehensive correlation of the term a as a function of temperature.

At operating temperatures other than the critical,

$$a(T) = a_C\,\alpha(T) \qquad (80)$$

where the temperature dependent function above is constrained by the limit $\alpha \rightarrow 1$ as $T \rightarrow T_C$. Values of α for a given substance were generated from vapor pressure data by numerical regression techniques. When values of $\alpha^{0.5}$ were then plotted against $1 - T_R^{0.5}$, nearly straight lines were obtained for a host of hydrocarbons. The result suggested the functional correlation form,

$$\alpha^{0.5} = 1 + m\left(1 - T_R^{0.5}\right) \;;\; T_R = T/T_C \qquad (81)$$

The slope m is a parameter characteristic of the component identity. It was successfully cross-correlated against the Pitzer acentric factor ω for a host of hydrocarbons. The "generalized" correlation assumed the form:

$$m = A + B\omega + C\omega^2 \qquad (82)$$

The coefficients to Equation 82 used in our work are different than those originally derived by Soave. We employed the modified coefficients developed by Graboski and Daubert (15) who used a more comprehensive vapor pressure data bank compiled by the American Petroleum Institute (API). Their recommended fit for m is,

$$m = 0.48508 + 1.55171\omega - 0.15613\omega^2 \qquad (83)$$

In his paper Soave recommends that Equation 75 be applied basically for non polar compounds. He warns that his equation is not accurate for polar substances like CO_2 and NH_3 or for quantum gases such as H_2.

The required pressure derivative functions and expressions for C_v and C_p based on the Soave equation are as follows.

$$\left(\frac{\partial P}{\partial T}\right)_V = \frac{R}{V-b} - \frac{da/dT}{V(V+b)} \quad ; \quad \left(\frac{\partial^2 P}{\partial T^2}\right)_V = -\frac{d^2a/dT^2}{V(V+b)}$$

$$\left(\frac{\partial P}{\partial V}\right)_T = -\frac{RT}{(V-b)^2} + \frac{a(2V+b)}{\left[V(V+b)\right]^2}$$

From Equation 48 we can now formulate the isochoric heat capacity departure function.

$$C_V - C_V^o = -T\int_{\infty}^{V} \frac{d^2a/dT^2}{V(V+b)}\,dV = -\frac{T}{b}\frac{d^2a}{dT^2}\,Ln\left[\frac{V}{V+b}\right] \;;\; C_V^o = C_P^o - R$$

Then from Equation 50, we obtain the relationship between C_p and C_v.

$$C_P - C_V = -T \frac{\left(\frac{R}{V-b} - \frac{da/dT}{V(V+b)} \right)^2}{\frac{a(2V+b)}{\left[V(V+b)\right]^2} - \frac{RT}{(V-b)^2}}$$

For a pure component the appropriate expressions for da/dT and da^2/dT^2 from the Soave equation become,

$$a = a_c \alpha = a_c \left[1 + m \left(1 - \left(\frac{T}{T_C} \right)^{0.5} \right) \right]^2$$

$$\frac{da}{dT} = 2a_c \left[1 + m \left(1 - \left(\frac{T}{T_C} \right)^{0.5} \right) \right] (-0.5m) \left(\frac{T^{-0.5}}{T_C^{0.5}} \right) = -\frac{a_c m \alpha^{0.5}}{\sqrt{T T_C}}$$

$$\frac{d^2 a}{dT^2} = -\frac{a_c m}{\sqrt{T_C}} \frac{d}{dT} \left[\frac{\alpha^{0.5}}{T^{0.5}} \right] = -\frac{a_c m}{\sqrt{T_C}} \left[\frac{0.5 \alpha^{-0.5}}{T^{0.5}} \frac{d\alpha}{dT} - \frac{0.5 \alpha^{0.5}}{T^{1.5}} \right]$$

$$\frac{d^2 a}{dT^2} = \frac{0.5 m a_c}{\sqrt{T T_C}} \left[\frac{\alpha^{0.5}}{T} - \frac{1}{\alpha^{0.5}} \frac{d\alpha}{dT} \right]$$

where it is quite clear that d α/ dT is given by

$$\frac{d\alpha}{dT} = -\frac{m \alpha^{0.5}}{\sqrt{T T_C}}$$

Peng-Robinson Equation Peng and Robinson of the University of Alberta (16) attempted to shore up some of the shortcomings of Soave's equation by amending the second term. They start out by writing,

$$P = P_R + P_A \qquad (84)$$

where the repulsive contribution (P_R) to the total pressure is,

$$P_R = \frac{RT}{V-b}$$

and the attractive portion (P_A) is expressed as,

$$P_A = -\frac{a}{g(V)}$$

The gist of Peng and Robinson's modification lies in the function g(V). They propose that,

$$g(V) = V(V+b) + b(V-b)$$

and therefore, Equation 84 may be written as,

$$P = \frac{RT}{V-b} - \frac{a(T)}{\left[V(V+b)+b(V-b)\right]} = \frac{RT}{V-b} - \frac{a(T)}{\left(V^2+2bV-b^2\right)} \qquad (85)$$

The term b(V - b) was not present in the original Soave equation. It was incorporated in order to improve the prediction of liquid density and produce a more realistic value for the universal critical compressibility factor. Once again, this equation can be put into the more convenient cubic form, explicit in Z.

$$Z^3 - (1-B)Z^2 + \left(A - 3B^2 - 2B\right)Z - \left(AB - B^2 - B^3\right) = 0 \qquad (86)$$

where

$$A = \frac{aP}{R^2T^2} \quad ; \quad a = a(T) \qquad (87)$$

$$B = \frac{bP}{RT} \quad ; \quad Z = \frac{PV}{RT} \qquad (88a,b)$$

$$a(T_C) = a_c = \frac{0.45724\,R^2T_C^2}{P_C} \qquad (89)$$

$$b(T_C) = b = \frac{0.07780\,RT_C}{P_C} \quad ; \quad Z_C = 0.307 \qquad (90a,b)$$

At temperatures other than T_C,

$$a(T) = a(T_C)\,\alpha\left(T_R, \omega\right) \tag{91}$$

$$b(T) = b(T_C) = b_c \text{ , no temperature dependency} \tag{92}$$

Using regression techniques with vapor pressure data, in a similar as did Soave, Peng and Robinson arrived at the following correlation for $\alpha(T_R,\omega)$.

$$\alpha^{0.5} = 1 + \kappa\left(1 - T_R^{0.5}\right) \tag{93}$$

$$\kappa = 0.37464 + 1.54226\,\omega - 0.26992\,\omega^2 \tag{94}$$

Both the Redlich-Kwong and Soave equations predict a universal Z_C of 0.333 whereas the Peng-Robinson equation yields a value of 0.307. This is a little more realistic in that the majority of hydrocarbons have a Z_C value of around 0.270.

Now, for evaluation of the JT coefficient, we need to first calculate the following thermodynamic properties directly from the Peng-Robinson equation:

$$\left(\frac{\partial P}{\partial T}\right)_V = \frac{R}{V-b} - \frac{da/dT}{V^2 + 2bV - b^2} \quad ; \quad \left(\frac{\partial^2 P}{\partial T^2}\right)_V = -\frac{d^2 a/dT^2}{V^2 + 2bV - b^2}$$

$$\left(\frac{\partial P}{\partial V}\right)_T = \frac{2a\left(V+b\right)}{\left(V^2 + 2bV - b^2\right)^2} - \frac{RT}{\left(V-b\right)^2}$$

Next the isochoric heat capacity departure for a Peng-Robinson fluid can be formulated from Equation 48.

$$C_V - C_V^o = -T\frac{d^2 a}{dT^2}\int_{\infty}^{V}\frac{dV}{V^2 + 2bV - b^2} = -T\,\frac{\dfrac{d^2 a}{dT^2}}{2\sqrt{2}\,b}\,Ln\left[\frac{V + b - \sqrt{2}\,b}{V + b + \sqrt{2}\,b}\right]$$

After substitution of the identities b = BRT/P and Z = PV/RT, the above expression assumes its final form,

$$C_V - C_V^o = -T\,\frac{d^2 a/dT^2}{2\sqrt{2}\,b}\,Ln\left[\frac{Z - 0.414\,B}{Z + 2.414\,B}\right]$$

where $C_V^o = C_P^o - R$

The value of C_P is then readily computed by substituting the above expressions for $(\partial P/\partial T)_V$ and $(\partial P/\partial V)_T$ into Equation 50. The Peng-Robinson expressions for d a/d T and d^2a/dT^2 are the same as those used for the Soave equation; however the term a_c is now calculated from Equation 89, and the term m is replaced by κ which in turn is computed via Equation 94.

Comparisons for Nitrogen In Table 3-155, page 3-110, Perry's Handbook (12) lists JT coefficient data for gaseous nitrogen over the following ranges of temperature and pressure:

	deg. C	deg. F
Temperature	- 150 to 300	- 238 to 572
	Atm	Psia
Pressure	1 To 200	14.7 to 2940

Table 4 of our paper here provides a detailed point-by-point comparison(1) between the measured JT data for gaseous nitrogen and the corresponding predictions of the four selected cubic equations of state. Table 5 shows the average prediction trends(1) for each level of pressure along with the overall average trends for the complete set of 122 data points. A summary of the overall trends is given below:

Eqn. of State	Avg. Trend, %
van der Waals	113.8
API Soave	-77.7
Redlich-Kwong	29.7
Peng-Robinson	39.0

A positive trend indicates that the equation being tested is predicting values of the JT coefficient that are too high on the average. Conversely, an overall negative trend indicates that the equation is predicting too low on the average.

The largest error trend of 113.8 percent is given by the VDW equation whereas the Redlich-Kwong equation produces the smallest average trend of 29.7 percent. An overall negative trend of -77.7 percent is generated from the API Soave equation. The Peng-Robinson yields about a 10 percent higher average trend than does the RK equation.

At the lower pressure levels, the experimental JT coefficients tend to decrease or become more negative as the temperature is increased. At the higher pressure levels, say at or above 100 atm, the JT coefficients tend to pass through a maximum value with increasing temperature. All four equations of state appear to at least capture this same general behavior.

Comparisons for Gaseous Carbon Dioxide In Table 3-153a, page 3-109 of Perry's Handbook, a total of 59 data points are listed for the JT coefficient of gaseous carbon dioxide. The following ranges of temperature and pressure are covered:

	deg. C	deg. F
Temperature	- 50 to 300	- 58 to 572
	Atm	Psia
Pressure	1 to 200	14.7 to 2940

(1) See the bottom of Tables 4 and 5 for the definition of point % deviation and average or overall trend in percent.

Table 6 lists all of the point-by-point comparisons between experimental and predicted JT coefficients. Table 7 summarizes the average deviation trends by pressure level, and also gives the overall error trends for all 59 data points. The overall error trends for each equation of state tested are summarized below:

Eqn. of State	Avg. Trend, %
van der Waals	-5.7
API Soave	-2.5
Redlich-Kwong	-1.7
Peng-Robinson	3.9

First of all, we point out that these error trends for carbon dioxide are at least an order of magnitude lower than those obtained for nitrogen. This is quite surprising in that CO_2 is a polar molecule and N_2 is non polar. Of the four equations tested the Redlich-Kwong generates the smallest trend of -1.7 percent, and the van der Waals equation produces the greatest overall trend of - 5.7 percent.

The JT coefficients for gaseous CO_2 basically follow a similar pattern as does N_2 with increasing temperature at the various pressure levels. At the lower pressure levels, the JT coefficients continuously decrease or become more negative with increasing temperature. At the higher pressures, values of the JT coefficient exhibit maxima as the temperature is increased. Both the measured and predicted JT coefficients exhibit this general overall behavior.

Comparisons for Liquid Carbon Dioxide Table 3-153a of Perry's Handbook also lists 20 measured JT coefficients for liquid CO_2 over the temperature range of - 75 to 0 deg. C and pressure range 20 to 200 atm. Table 8 shows all of the point-by-point comparisons between predicted and experimental JT coefficients. Most of the coefficients shown here assume negative values. Therefore, we have expressed each point comparison as an absolute percent deviation, namely,

$$Abs\,\%\,Dev = ABS\left[\frac{\mu_{JT-\mathrm{Pred.}} - \mu_{JT-Exper.}}{\mu_{JT-Exper.}}(100)\right]$$

As a result, each point percent deviation is always a positive number. Summarized at the bottom of Table 8 are the overall absolute average deviations produced by each equation for the entire data set. They are as follows:

Eqn. of State	Overall Abs. Avg. Dev, %
van der Waals	290.5
API Soave	33.5
Redlich-Kwong	36.5
Peng-Robinson	34.8

The van der Waals equation produces an overall absolute deviation of nearly 300 percent. The other three equations produce comparable absolute average deviations of around 35 percent on the average.

Illustration 8 Based on an enthalpy-temperature diagram for **ethylene** developed from the data of York and White (17) and Benzler and Koch (18), the following isenthalpic T-P points were read over the pressure range 800 to 15,000 psia:

At H = 1040 Btu/Lb*

Press., Psia	Temp., deg. F
800	52
1000	62
1200	72
1500	82
2000	92
2500	96
5000	105
10,000	87
15,000	58

* The enthalpy datum for this H-T chart is H^o = 1000 Btu/Lb in the ideal gas state at a reference temperature of 0 deg. R.

We are asked to see if the above data can be fit with reasonable accuracy to an analytical equation (T = f(P)). If such a fit is successful, we are then asked to calculate (predict) the inversion point if one exists. Finally, it is desired to derive values for the JT coefficient from the above equation fit.

Figure 20 is a basic plot of the above isenthalpic T-P data. The plot shows a maximum at approximately a pressure slightly below 5000 psia. We attempted to perform quadratic and hyperbolic equation regression fits of this curve with little success.

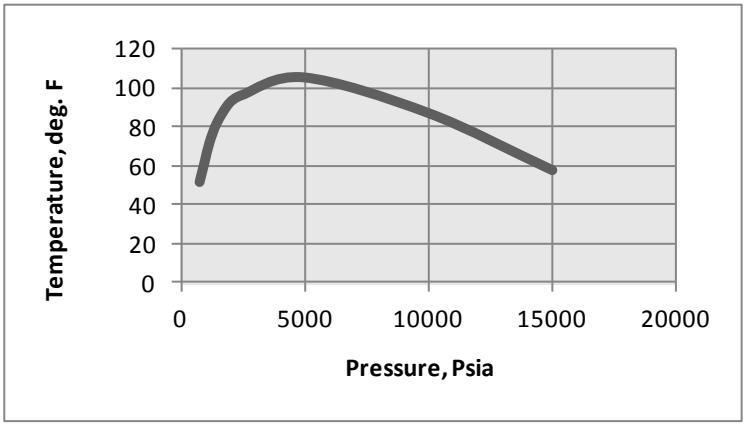

Figure 20. Ethylene Isenthalpic T-P Data.

However, when the data were plotted on a log-log scale, a quadratic equation of the form,

$$LnT = A(LnP)^2 + B\,LnP + C \qquad (95)$$

could successfully be fitted via the method of least-squares. The plot and resulting equation fit are displayed in Figure 21. The coefficients to Equation 95 turn out to be

A = -0.2946 ; B = 4.861 ; C = - 15.392

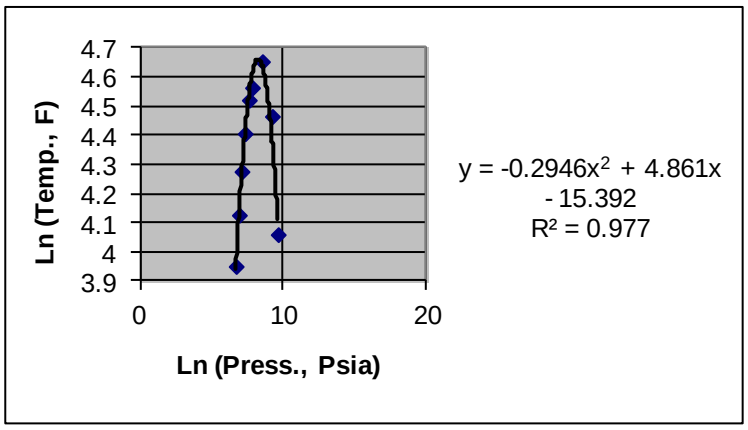

Figure 21. Ethylene Isenthalpic T-P Data (Log-Log Scale).

Equation 95 predicts the isenthalpic temperatures for all nine data points with an average error trend of only - 0.11 percent. The corresponding expression for the JT coefficient is readily derived by differentiating Equation 95 as follows:

$$\frac{d\,LnT}{d\,P} = \frac{1}{T}\frac{d\,T}{d\,P} = 2\,A\left(Ln\,P\right)\frac{1}{P} + \frac{B}{P}$$

or

$$\mu_{JT} = \left(\frac{\partial T}{\partial P}\right)_H = \frac{T}{P}\left[2\,A(Ln\,P) + B\ \right] \quad (96)$$

In all of these expressions, the pressure is in units of psia and the temperature in deg. F. The inversion temperature and pressure can be estimated as follows:

First set $\mu_{JT} = 0$ in Equation 96 and solve for the inversion pressure with the result,

$$2\,A\,Ln\,P + B = 0$$

or

$$Ln\,P = -\frac{B}{2\,A} = -\frac{4.861}{(2)(-0.2946)} = 8.2502$$

whereby

$$P = 3828.28\ Psia$$

The inversion temperature is readily calculated by substituting the above inversion pressure directly back into Equation 95,

$$LnT = -0.2946(8.2502)^2 + 4.861(8.2502) - 15.392$$

$$LnT = 4.66004$$

$$T = 105.6\ \text{deg}.F \quad \max.T$$

This represents the inversion temperature which is the maximum temperature on the isenthalpic curve. And finally, we can substitute the observed values of pressure directly into Equation 96 in order to generate values for the JT coefficient.

These predicted values are summarized below:

Press., Psia	Eqn. 95 Calc. Temp., F.	Eqn. 96 JT Coeff, (^{o}F/Psia)
800	51.3	0.0592
1000	62.1	0.0491
1200	71.1	0.0405
1500	81.6	0.0300
2000	93.3	0.0178
2500	100.1	0.0101
5000	103.4	- 0.0033
10,000	80.5	- 0.0046
15,000	61.0	- 0.0033

Figure 22 shows the plot of these predicted JT coefficients against pressure.

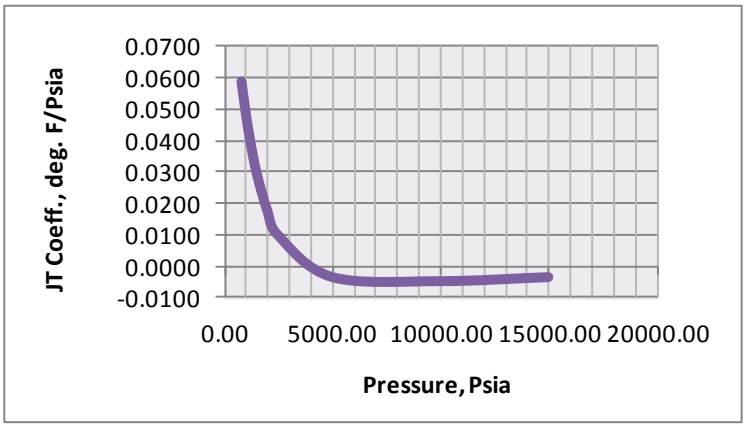

Figure 22. Calculated JT Coefficients for C_2H_4.

References

1. Lee, B. I. L. and Kesler, M. G., AI Ch E Journal, **21**, No. 3, 510 (May, 1975)

2. Pitzer, K.S. and Curl, R.F. Jr., Journ. Am. Chem. Soc., **77**, 3433 (1955).

3. IBID, **79**, 2369 (1957).

4. Curl, R.F. and Pitzer, K.S., Ind. Eng. Chem., **50**, 265 (1958).

5. Data Book of the American Petroleum Institute (API), Procedure 7A1.1.

6. Keenan, Keyes, Hill and Moore, Steam Tables, John Wiley & Sons, (1969) (Table 4, Pages 104-107).

7. Moore, W.J., Physical Chemistry, 3rd Ed., Prentice-Hall, Inc. (1962) Page 43.

8. Zemansky, M.W., Heat and Thermodynamics, 4th Ed., McGraw-Hill Book Co., (1957) Page 282.

9. Sandler, S.I., Chemical and Engineering Thermodynamics, John Wiley & Sons, (1977) Page 221.

10. Dymond, J.H. and Smith, E.B., The Virial Coefficients of Gases, Clarendon Press, Oxford (1969) Page 188.

11. Miller, D.G. Ind. Eng. Chem. Fundam., **9**, No. 4 (1970) Page 585.

12. Perry, R.H. Perry's Chemical Engineers' Handbook, 6th Ed., McGraw-Hill Book Co., (1984) Pages 3-107 to 3-110.

13. Redlich, O. and Kwong, J.N.S. Chemical Reviews, **44**, (1949) Page 233.

14. Soave, G. Chem. Eng. Sci., **27**, (1972) Page 1197.

15. Graboski, M.S. and Daubert, T.E., Ind. Eng. Chem. Proc. Des. Dev., **17**, No.4 (1978) Page 443.

16. Peng, D.Y. and Robinson, D.B., Ind. Eng. Chem. Fundam., **15**, No. 1, (1976) Page 59.

17. York and White, Trans. Am. Inst. Chem. Engrs., **40**, (1944) Page 227.

18. Benzler and Koch, Chem. Ing. Tech., **27**, (1955) Pages 72-73.

Appendix of Tables

Table 1. Coefficients for Equations 14, 15 and 16 - Ideal Gas Enthalpy, Entropy

	Component Name	A*	B	Cx10**4	Dx10**7	Ex10**11	Fx10**15	G*	Applicable Temperature Range, deg. F
Nonhydrocarbons	Hydrogen	12.32674	3.199617	3.927862	-2.93452	10.90069	-13.87867	-4.938247	-280 to 2200
	Nitrogen	-0.93401	0.255204	-0.17794	0.158913	-0.32203	0.158927	0.042363	-280 to 2200
	Oxygen	-0.98176	0.227486	-0.37305	0.483017	-1.852433	2.474881	0.124314	-280 to 2200
	Water	-2.46342	0.457392	-0.525117	0.645939	-2.027592	2.363096	-0.33983	-280 to 2200
	Carbon Monoxide	-0.97557	0.256524	-0.229112	0.222803	-0.563256	0.455878	0.09247	-280 to 2200
	Carbon Dioxide	4.77805	0.114433	1.011325	-0.264936	0.347063	-0.1314	0.343357	-280 to 2200
	Ammonia	-0.94695	0.480156	-0.86258	1.74952	-6.54285	8.55687	-0.284511	-280 to 2200
	Hydrogen Sulfide	-0.61782	0.238575	-0.244571	0.410673	-1.301258	1.44852	-0.045932	-280 to 2200
	Sulfur Dioxide	1.39432	0.110263	0.33029	0.089125	-0.773135	1.292865	0.194798	-280 to 2200
Paraffins	Methane	-6.97702	0.571700	-2.943122	4.231568	-15.2674	19.45261	-0.656038	-280 to 2200
	Ethane	-0.02121	0.264878	-0.25014	2.923341	-12.86053	18.22057	0.082172	-280 to 2200
	Propane	-0.73842	0.172601	0.94041	2.155433	-10.7099	15.92794	0.206577	-280 to 2200
	n-butane	7.43041	0.098571	2.691795	0.516202	-4.20139	6.560421	0.351649	-100 to 2200
	n-pentane	27.17183	-0.002795	4.400733	-0.862875	0.817644	-0.197154	0.736161	0 to 2200
	n-hexane	-7.39083	0.229107	-0.815691	4.527826	-25.23179	47.4802	-0.422963	-100 to 1300
	n-heptane	-0.06609	0.180209	0.347292	3.218786	-18.36603	33.76938	-0.253997	-100 to 1300
	n-octane	1.11983	0.173084	0.488101	3.054008	-17.36547	31.24831	-0.26234	-100 to 1300
	n-nonane	1.71981	0.169056	0.581255	2.926114	-16.5585	29.29609	-0.276768	-100 to 1300
	n-decane	-2.99313	0.203347	-0.349035	4.070565	-23.06441	42.96897	-0.456882	-100 to 1300
Naphthenes	Cyclopentane	57.78000	-0.174553	4.878999	-0.790213	-0.259001	1.873384	1.606204	0 to 2200
	Methylcyclopentane	54.70525	-0.163500	5.315238	-1.23976	1.465505	-0.497681	1.473383	0 to 2200
	Cyclohexane	46.56603	-0.149848	4.572747	-0.387392	-1.791242	3.793529	1.318154	0 to 2200
	Methylcyclohexane	46.25893	-0.168390	5.444843	-1.126886	0.751131	0.606023	1.357148	0 to 2200
Olefins	Ethylene	25.83557	0.144963	1.710121	0.761974	-4.503085	6.664928	0.748330	0 to 2200
	Propylene	28.53396	0.030810	3.512242	-0.494661	-0.226171	1.125539	0.965351	0 to 2200
	1-butene	32.74090	-0.018519	4.263451	-0.940582	1.072240	-0.349830	0.999353	0 to 2200
	Isobutylene	14.96746	0.033009	3.782637	-0.733312	0.697566	-0.174830	0.867557	0 to 2200
Diolefins and Acetylenes	Propadiene	25.33539	0.033745	3.715168	-1.062607	1.864623	-1.435039	0.886725	0 to 2200
	1,3-butadiene	40.76384	-0.100603	5.651872	-2.123463	4.830541	-4.738449	1.339874	0 to 2200
	Acetylene	35.24627	0.022636	5.459217	-2.976556	8.738401	-10.045390	1.226331	0 to 2200
	Propyne	15.21043	0.080387	3.240066	-0.879745	1.599146	-1.400978	0.662198	0 to 2200
Aromatics	Benzene	36.31430	-0.122662	4.310824	-1.138140	1.494985	-0.564766	1.178204	0 to 2200
	Toluene	31.88489	-0.101151	4.225723	-1.061438	1.337653	-0.484075	1.054833	0 to 2200
	Ethyl benzene	30.33272	-0.093633	4.390839	-1.126299	1.458215	-0.543200	0.974441	0 to 2200
	O-xylene	13.97958	-0.014950	3.342431	-0.484082	-0.460172	1.705569	0.551212	0 to 2200

* Base levels are H = 0 for the ideal gas state at 0 deg. R and S = 0 for the ideal gas at 0 deg. R and a reference pressure of 1 atm.

Table 2. Summary of Approximate Inversion-Curves for Several Components as Reported in Perry's Handbook - 6th Edition (1978) Pages 3-107 Through 3-110 (12)

Approximate Inversion-Curve Locus for Air

P, bar	0	25	50	75	100	125	150	175	200	225
TL, deg. K	112	114	117	120	124	128	132	137	143	149
TU, deg. K	653	641	629	617	606	594	582	568	555	541

P, bar	250	275	300	325	350	375	400	425	432
TL, deg. K	156	164	173	184	197	212	230	265	300
TU, deg. K	526	509	491	470	445	417	386	345	300

Approximate Inversion-Curve Locus for Argon

P, bar	0	25	50	75	100	125	150	175	200	225
TL, deg. K	94	97	101	105	109	113	118	123	128	134
TU, deg. K	765	755	744	736	726	716	705	694	683	671

P, bar	250	275	300	325	350	375	400	425	450	475
TL, deg. K	141	148	158	170	183	201	222	248	288	375
TU, deg. K	657	643	627	610	591	569	544	515	478	375

Approximate Inversion-Curve Locus for Carbon Dioxide

P, bar	50	100	150	200	250	300	350	400	450
TL, deg. K	243	251	258	266	272	283	293	302	312
TU, deg. K	1290	1261	1233	1205	1175	1146	1146	1076	1045

P, bar	500	550	600	650	700	750	800	850	884
TL, deg. K	325	338	351	365	383	403	441	496	608
TU, deg. K	1015	983	950	914	878	840	796	739	608

Approximate Inversion-Curve Locus for Deuterium

P, bar	0	25	50	75	100	125	150	175	194
TL, deg. K	31	34	38	43	49	56	65	77	108
TU, deg. K	216	202	189	178	168	157	146	131	108

Table 2 (Cont). Summary of Approximate Inversion-Curves for Several Components as Reported in Perry's Handbook - 6th Edition (1978) Pages 3-107 Through 3-110 (12)

Approximate Inversion-Curve Locus for Normal Hydrogen

P, bar	0	25	50	75	100	125	150	164
TL, deg. K	28	32	38	44	52	61	73	92
TU, deg. K	202	193	183	171	157	141	119	92

Approximate Inversion-Curve Locus for Methane

P, bar	25	50	75	100	125	150	175	200	225	250	275	300
TL, deg. K	-	161	166	172	176	182	189	195	202	209	217	225

P, bar	325	350	375	400	425	450	475	500	525	534
TL, deg. K	234	243	254	265	277	292	309	331	365	400
TU, deg. K	-	-	-	-	-	-	505	474	437	400

Approximate Inversion-Curve Locus for Ethane
Lower Inversion Curve Only

P, bar	0	25	50	75	100	125	150	175	200	225
TL, deg. K	-	249	255	262	269	275	282	290	297	306

P, bar	250	275	300	325	350	375	400	425	450	475
TL, deg. K	315	325	335	345	357	370	383	398	415	432

P, bar	500	525	550	575	600
TL, deg. K	453	477	505	545	626

Approximate Inversion-Curve Locus for Propane
Lower Inversion Curve Only

P, bar	0	25	50	75	100	125	150	175	200	225	250	275
TL, deg. K	296	303	311	318	327	336	345	355	365	374	389	403

P, bar	300	325	350	375	400	425	450	475	500	525	541
TL, deg. K	418	435	452	473	495	521	551	586	628	686	780

Table 3. Critical Constants for Inversion Curve Components.

Component	Critical Pressure	Critical Temperature	Acentric
	Psia	Bars	deg. F	deg. K	Factor
Hydrogen*	188.2	12.98	-399.8	33.28	0.00
Argon	705.6	48.65	-188.4	150.72	0.00
Nitrogen	493	33.99	-232.4	126.28	0.045
Oxygen	737.1	50.82	-181.1	154.78	0.019
Air**	544.3	37.52	-221.6	132.26	0.040
Carbon Dioxide	1070.6	73.81	87.9	304.22	0.231
Methane	667.8	46.04	-116.6	190.61	0.0104
Ethane	707.8	48.80	90.1	305.44	0.0986
Propane	616.3	42.49	206.0	369.83	0.1524

* Classical Critical Constants

** Composition of air is assumed to be 79 vol % N2/ 21 vol % O2

Table 4. Comparison of Predicted and Experimental Joule-Thomson Coefficients for Gaseous Nitrogen.

Temp. deg. C	Temp. deg. F	Press. Atm	Press. Psia	Measured* JT Coeff. deg. C/Atm	Measured* JT Coeff. deg. F/Psia	Predicted JT Coeff. Orig. VDW Eqn. deg. F/Psia	% Dev**	Predicted JT Coeff. API Soave deg. F/Psia	% Dev**	Predicted JT Coeff. Redlich-Kwong deg. F/Psia	% Dev**	Predicted JT Coff. Peng-Robinson deg. F/Psia	% Dev**
-150	-238	1	14.7	1.2659	0.1551	0.0980	-36.8	0.1373	-11.4	0.1345	-13.3	0.1416	-8.7
-125	-193	1	14.7	0.8557	0.1048	0.0785	-25.1	0.1031	-1.6	0.0991	-5.4	0.1083	3.3
-100	-148	1	14.7	0.6490	0.0795	0.0647	-18.6	0.0798	0.4	0.0761	-4.3	0.0855	7.6
-75	-103	1	14.7	0.5033	0.0616	0.0545	-11.6	0.0629	2.0	0.0601	-2.5	0.0690	11.9
-50	-58	1	14.7	0.3968	0.0486	0.0465	-4.3	0.0502	3.3	0.0485	-0.2	0.0564	16.0
-25	-13	1	14.7	0.3224	0.0395	0.0401	1.5	0.0404	2.3	0.0397	0.5	0.0467	18.3
0	32	1	14.7	0.2656	0.0325	0.0349	7.3	0.0326	0.2	0.0328	0.8	0.0389	19.6
25	77	1	14.7	0.2217	0.0272	0.0306	12.7	0.0263	-3.1	0.0273	0.5	0.0325	19.7
50	122	1	14.7	0.1855	0.0227	0.0269	18.4	0.0211	-7.1	0.0229	0.8	0.0272	19.7
75	167	1	14.7	0.1555	0.0190	0.0238	25.0	0.0168	-11.8	0.0192	0.8	0.0229	20.2
100	212	1	14.7	0.1292	0.0158	0.0210	32.7	0.0132	-16.6	0.0162	2.4	0.0191	20.7
125	257	1	14.7	0.1070	0.0131	0.0186	41.9	0.0101	-22.9	0.0136	3.8	0.0159	21.3
150	302	1	14.7	0.0868	0.0106	0.0165	55.2	0.00745	-29.9	0.0114	7.2	0.0131	23.2
200	392	1	14.7	0.0558	0.0068	0.0130	90.2	0.00322	-52.9	0.00784	14.7	0.00864	26.4
250	482	1	14.7	0.0331	0.0041	0.0101	149.1	0.0000234	-99.4	0.00514	26.8	0.00519	28.0
300	572	1	14.7	0.0140	0.0017	0.00775	352.0	-0.00243	-241.7	0.00303	76.7	0.00249	45.2
				N = 16	Avg. Trend, % =		43.1		-30.6		6.8		18.3
-150	-238	20	294	1.1246	0.1377	0.1259	-8.6	0.1461	6.1	0.1421	3.2	0.1491	8.2
-125	-193	20	294	0.7948	0.0973	0.0873	-10.3	0.0997	2.4	0.0966	-0.8	0.1038	6.6
-100	-148	20	294	0.5958	0.0730	0.0677	-7.2	0.0746	2.2	0.0721	-1.2	0.0792	8.5
-75	-103	20	294	0.4671	0.0572	0.0551	-3.7	0.0580	1.4	0.0563	-1.6	0.0630	10.1
-50	-58	20	294	0.3734	0.0457	0.0461	0.8	0.0460	0.6	0.0451	-1.4	0.0512	11.9
-25	-13	20	294	0.3013	0.0369	0.0393	6.5	0.0369	0.0	0.0368	-0.3	0.0423	14.6
0	32	20	294	0.2494	0.0305	0.0339	11.0	0.0297	-2.8	0.0304	-0.5	0.0352	15.2
25	77	20	294	0.2060	0.0252	0.0295	16.9	0.0239	-5.3	0.0253	0.3	0.0294	16.5
50	122	20	294	0.1709	0.0209	0.0258	23.3	0.0192	-8.3	0.0211	0.8	0.0246	17.5
75	167	20	294	0.1421	0.0174	0.0227	30.4	0.0152	-12.7	0.0177	1.7	0.0206	18.4
100	212	20	294	0.1173	0.0144	0.0200	39.2	0.0119	-17.2	0.0149	3.7	0.0172	19.7
125	257	20	294	0.0973	0.0119	0.0176	47.7	0.00901	-24.4	0.0125	4.9	0.0143	20.0
150	302	20	294	0.0776	0.0095	0.0156	64.1	0.00657	-30.9	0.0104	9.4	0.0118	24.2
200	392	20	294	0.0472	0.0058	0.0122	111.0	0.00262	-54.7	0.00707	22.3	0.00768	32.8
250	482	20	294	0.0256	0.0031	0.0094	199.8	-0.000389	-112.4	0.00452	44.2	0.00448	42.9
300	572	20	294	0.0096	0.0012	0.0071	503.8	-0.00271	-330.5	0.00253	115.2	0.00197	67.5
				N = 16	Avg. Trend, % =		64.0		-36.6		12.5		20.9

Table 4 (Cont.). Comparison of Predicted and Experimental Joule-Thomson Coefficients for Gaseous Nitrogen.

-125	-193	33.5	492	0.7025	0.0860	0.0931	8.2	0.0927	7.7	0.0908	5.5	0.0953	10.8
-100	-148	33.5	492	0.5494	0.0673	0.0688	2.2	0.0693	3.0	0.0678	0.8	0.0730	8.5
-75	-103	33.5	492	0.4318	0.0529	0.0548	3.6	0.0539	1.9	0.0529	0.0	0.0581	9.9
-50	-58	33.5	492	0.3467	0.0425	0.0453	6.7	0.0428	0.8	0.0424	-0.2	0.0474	11.6
-25	-13	33.5	492	0.2854	0.0350	0.0383	9.6	0.0344	-1.6	0.0346	-1.0	0.0391	11.9
0	32	33.5	492	0.2377	0.0291	0.0329	13.0	0.0277	-4.9	0.0286	-1.8	0.0326	12.0
25	77	33.5	492	0.1961	0.0240	0.0285	18.7	0.0223	-7.2	0.0238	-0.9	0.0273	13.7
50	122	33.5	492	0.1621	0.0199	0.0249	25.4	0.0179	-9.8	0.0199	0.2	0.0229	15.3
75	167	33.5	492	0.1336	0.0164	0.0218	33.2	0.0141	-13.8	0.0167	2.1	0.0192	17.3
100	212	33.5	492	0.1100	0.0135	0.0192	42.5	0.01098	-18.5	0.0140	3.9	0.0160	18.8
125	257	33.5	492	0.0904	0.0111	0.0169	52.6	0.00829	-25.1	0.0117	5.7	0.0133	20.1
150	302	33.5	492	0.0734	0.0090	0.0149	65.7	0.00597	-33.6	0.00971	8.0	0.0109	21.2
200	392	33.5	492	0.0430	0.0053	0.0116	120.3	0.00221	-58.0	0.00654	24.2	0.00704	33.7
250	482	33.5	492	0.0230	0.0028	0.00888	215.2	-0.000667	-123.7	0.00410	45.5	0.00401	42.3
300	572	33.5	492	0.0050	0.00061	0.00669	992.4	-0.00290	-573.5	0.00219	257.6	0.00162	164.5
				N=15	Avg. Trend, % =		107.3		-57.1		23.3		27.4

* Table 264, Smithsonian Physical Tables, 9th rev. ed., Washington, DC, 1954.

** % Dev. = 100*(JT-pred - JT-meas)/JT-meas

Table 4 (Cont.). Comparison of Predicted and Experimental Joule-Thomson Coefficients for Gaseous Nitrogen.

Temp. deg. C	Temp. deg. F	Press. Atm	Press. Psia	Measured* JT Coeff. deg. C/Atm	Measured* JT Coeff. deg. F/Psia	Predicted JT Coeff. Orig. VDW Eqn. deg. F/Psia	% Dev**	Predicted JT Coeff. API Soave deg. F/Psia	% Dev**	Predicted JT Coeff. Redlich-Kwong deg. F/Psia	% Dev**	Predicted JT Coeff. Peng-Robinson deg. F/Psia	% Dev**
-125	-193	60	882	0.4940	0.0605	0.0558	-7.8	0.0578	-4.5	0.0570	-5.8	0.0581	-4.0
-100	-148	60	882	0.4506	0.0552	0.0620	12.3	0.0550	-0.3	0.0547	-0.9	0.0568	2.9
-75	-103	60	882	0.3712	0.0455	0.0505	11.1	0.0448	-1.5	0.0447	-1.7	0.0476	4.7
-50	-58	60	882	0.3059	0.0375	0.0418	11.6	0.0363	-3.1	0.0365	-2.6	0.0396	5.7
-25	-13	60	882	0.2528	0.0310	0.0353	14.0	0.0294	-5.0	0.0301	-2.8	0.0331	6.9
0	32	60	882	0.2088	0.0256	0.0302	18.1	0.0238	-6.9	0.0250	-2.2	0.0278	8.7
25	77	60	882	0.1729	0.0212	0.0261	23.2	0.0193	-8.9	0.0208	-1.8	0.0234	10.5
50	122	60	882	0.1449	0.0177	0.0227	27.9	0.0154	-13.2	0.0174	-2.0	0.0197	11.0
75	167	60	882	0.1191	0.0146	0.0199	36.4	0.0122	-16.4	0.0146	0.1	0.0165	13.1
100	212	60	882	0.0975	0.0119	0.0174	45.7	0.00937	-21.5	0.0122	2.2	0.0138	15.6
125	257	60	882	0.0786	0.0096	0.0153	58.9	0.00696	-27.7	0.0102	6.0	0.0114	18.4
150	302	60	882	0.0628	0.0077	0.0135	75.5	0.00488	-36.6	0.00840	9.2	0.00933	21.3
200	392	60	882	0.0372	0.0046	0.0103	126.1	0.00146	-68.0	0.00552	21.1	0.00588	29.1
250	482	60	882	0.0160	0.0020	0.00785	300.6	-0.00118	-160.2	0.00330	68.4	0.00315	60.7
300	572	60	882	-0.0013	-0.00016	0.00580	3724.5	-0.00325	-1931.7	0.00155	1068.3	0.000972	707.0
			N = 15		Avg. Trend, % =		298.5		-153.7		77.0		60.8
-125	-193	100	1470	0.1314	0.01609	0.00884	-45.1	0.0189	17.4	0.0173	7.5	0.0195	21.2
-100	-148	100	1470	0.2754	0.03373	0.02604	-22.8	0.0315	-6.6	0.0303	-10.2	0.0322	-4.5
-75	-103	100	1470	0.2682	0.03285	0.03272	-0.4	0.0309	-5.9	0.0305	-7.2	0.0323	-1.7
-50	-58	100	1470	0.2332	0.02856	0.03120	9.2	0.0268	-6.2	0.0270	-5.5	0.0289	1.2
-25	-13	100	1470	0.2001	0.02451	0.02785	13.6	0.0225	-8.2	0.0231	-5.7	0.0251	2.4
0	32	100	1470	0.1679	0.02056	0.02448	19.0	0.0186	-9.6	0.0196	-4.7	0.0215	4.5
25	77	100	1470	0.1400	0.01715	0.02147	25.2	0.0151	-11.9	0.0166	-3.2	0.0183	6.7
50	122	100	1470	0.1164	0.01426	0.01882	32.0	0.0121	-15.1	0.0139	-2.5	0.0155	8.7
75	167	100	1470	0.0941	0.01153	0.01652	43.3	0.00949	-17.7	0.0117	1.5	0.0131	13.7
100	212	100	1470	0.0768	0.00941	0.01450	54.1	0.00720	-23.5	0.00972	3.3	0.0109	15.9
125	257	100	1470	0.0621	0.00761	0.01271	67.1	0.00518	-31.9	0.00802	5.4	0.00896	17.8
150	302	100	1470	0.0482	0.00590	0.01113	88.5	0.00341	-42.2	0.00654	10.8	0.00724	22.6
200	392	100	1470	0.0262	0.00321	0.008449	163.3	0.000455	-85.8	0.00410	27.8	0.00434	35.2
250	482	100	1470	0.0071	0.00087	0.006265	620.4	-0.00188	-316.2	0.00217	149.5	0.00201	131.1
300	572	100	1470	-0.0075	-0.00092	0.004458	584.4	-0.00373	-305.6	0.000640	169.4	0.000112	112.0
			N=15		Avg. Trend, % =		110.1		-57.9		22.4		25.8

Table 4 (Cont.). Comparison of Predicted and Experimental Joule-Thomson Coefficients for Gaseous Nitrogen.

-125	-193	140	2057	0.0498	0.00610	-0.00125	-120.5	0.00845	38.5	0.00720	18.0	0.00910	49.2
-100	-148	140	2057	0.1373	0.01682	0.007220	-57.1	0.0169	0.5	0.0153	-9.0	0.0176	4.7
-75	-103	140	2057	0.1735	0.02125	0.01474	-30.6	0.0199	-6.4	0.0189	-11.1	0.0209	-1.7
-50	-58	140	2057	0.1676	0.02053	0.01826	-11.0	0.0190	-7.4	0.0186	-9.4	0.0204	-0.6
-25	-13	140	2057	0.1506	0.01845	0.01864	1.1	0.0167	-9.5	0.0169	-8.4	0.0185	0.3
0	32	140	2057	0.1316	0.01612	0.01760	9.2	0.0141	-12.5	0.0148	-8.2	0.0163	1.1
25	77	140	2057	0.1105	0.01353	0.01607	18.7	0.0116	-14.3	0.0127	-6.2	0.0141	4.2
50	122	140	2057	0.0915	0.01121	0.01443	28.8	0.00931	-16.9	0.0107	-4.5	0.0121	8.0
75	167	140	2057	0.0740	0.00906	0.01283	41.6	0.00721	-20.5	0.00901	-0.6	0.0102	12.5
100	212	140	2057	0.0582	0.00713	0.01134	59.1	0.00533	-25.2	0.00746	4.7	0.00846	18.7
125	257	140	2057	0.0459	0.00562	0.009969	77.3	0.00365	-35.1	0.00608	8.1	0.00690	22.7
150	302	140	2057	0.0348	0.00426	0.008712	104.4	0.00214	-49.8	0.00486	14.0	0.00548	28.6
200	392	140	2057	0.0168	0.00206	0.006514	216.6	-0.000428	-120.8	0.00280	36.1	0.00304	47.7
250	482	140	2057	0.0009	0.00011	0.004674	4140.1	-0.00249	-2358.8	0.00114	934.2	0.00103	834.4
300	572	140	2057	-0.0129	-0.00158	0.003122	297.6	-0.00416	-163.3	-0.000193	87.8	-0.000634	59.9
			N = 15		Avg. Trend, % =		318.3		-186.8		69.7		72.6

* Table 264, Smithsonian Physical Tables, 9th rev. ed., Washington, DC, 1954.

** % Dev. = 100*(JT-pred - JT-meas)/JT-meas

Table 4 (Cont.). Comparison of Predicted and Experimental Joule-Thomson Coefficients.

Temp. deg. C	Temp. deg. F	Press. Atm	Press. Psia	Measured* JT Coeff. deg. C/Atm	Measured* JT Coeff. deg. F/Psia	Predicted JT Coeff. Orig. VDW Eqn. deg. F/Psia	% Dev**	Predicted JT Coeff. API Soave deg. F/Psia	% Dev**	Predicted JT Coeff. Redlich-Kwong deg. F/Psia	% Dev**	Predicted JT Coff. Peng-Robinson deg. F/Psia	% Dev**
-125	-193	180	2645	0.0167	0.0020	-0.005678	-377.6	0.00385	88.2	0.00288	40.8	0.00451	120.5
-100	-148	180	2645	0.0765	0.0094	-0.0006752	-107.2	0.00935	-0.2	0.00782	-16.5	0.0101	7.8
-75	-103	180	2645	0.1026	0.0126	0.004486	-64.3	0.0125	-0.5	0.0112	-10.9	0.0134	6.6
-50	-58	180	2645	0.1120	0.0137	0.008362	-39.0	0.0130	-5.2	0.0122	-11.1	0.0142	3.5
-25	-13	180	2645	0.1101	0.0135	0.01039	-23.0	0.0120	-11.0	0.0117	-13.2	0.0135	0.1
0	32	180	2645	0.1015	0.0124	0.01097	-11.8	0.0104	-16.3	0.0106	-14.7	0.0122	-1.9
25	77	180	2645	0.0874	0.0107	0.01070	0.0	0.00868	-18.9	0.00930	-13.1	0.0108	0.9
50	122	180	2645	0.0732	0.0090	0.01001	11.6	0.00693	-22.7	0.00794	-11.4	0.00925	3.2
75	167	180	2645	0.0583	0.0071	0.009125	27.8	0.00527	-26.2	0.00665	-6.9	0.00780	9.2
100	212	180	2645	0.0462	0.0057	0.008174	44.5	0.00373	-34.1	0.00544	-3.9	0.00643	13.6
125	257	180	2645	0.0347	0.0043	0.007221	69.9	0.00231	-45.6	0.00434	2.1	0.00516	21.4
150	302	180	2645	0.0248	0.0030	0.006300	107.4	0.00103	-66.1	0.00334	10.0	0.00398	31.0
200	392	180	2645	0.0094	0.0012	0.004600	299.5	-0.00120	-204.2	0.00162	40.7	0.00191	65.9
250	482	180	2645	-0.0037	-0.0005	0.003108	712.2	-0.00304	-517.4	0.000204	131.4	0.000174	125.4
300	572	180	2645	-0.0160	-0.0020	0.001813	188.6	-0.00454	-129.0	-0.000957	50.1	-0.00129	33.5
			N = 15		Avg. Trend, % =		55.9		-67.3		11.6		29.4
-125	-193	200	2939	0.0032	0.0004	-0.00708	-1906.4	0.00239	509.8	0.00154	292.9	0.00305	678.2
-100	-148	200	2939	0.0587	0.0072	-0.003034	-142.2	0.00694	-3.5	0.00549	-23.6	0.00771	7.2
-75	-103	200	2939	0.0800	0.0098	0.001247	-87.3	0.00990	1.0	0.00846	-13.7	0.0108	10.2
-50	-58	200	2939	0.0906	0.0111	0.004796	-56.8	0.0107	-3.6	0.00968	-12.8	0.0118	6.3
-25	-13	200	2939	0.0932	0.0114	0.007036	-38.4	0.0101	-11.5	0.00960	-15.9	0.0115	0.7
0	32	200	2939	0.0891	0.0109	0.008058	-26.2	0.00889	-18.5	0.00885	-18.9	0.0105	-3.8
25	77	200	2939	0.0779	0.0095	0.008240	-13.6	0.00741	-22.3	0.00782	-18.0	0.00932	-2.3
50	122	200	2939	0.0666	0.0082	0.007928	-2.8	0.00589	-27.8	0.00669	-18.0	0.00804	-1.4
75	167	200	2939	0.0543	0.0067	0.007351	10.5	0.00441	-33.7	0.00558	-16.1	0.00676	1.6
100	212	200	2939	0.0419	0.0051	0.006645	29.5	0.00301	-41.3	0.00453	-11.7	0.00554	7.9
125	257	200	2939	0.0326	0.0040	0.005890	47.5	0.00172	-56.9	0.00355	-11.1	0.00439	9.9
150	302	200	2939	0.0228	0.0028	0.005127	83.6	0.000527	-81.1	0.00265	-5.1	0.00332	18.9
200	392	200	2939	0.0070	0.0009	0.003666	327.6	-0.00156	-282.0	0.00107	24.8	0.00141	64.5
250	482	200	2939	-0.0058	-0.0007	0.002344	436.3	-0.00329	-368.5	-0.000232	68.3	-0.000210	71.5
300	572	200	2939	-0.0171	-0.0021	0.001174	155.6	-0.00472	-125.0	-0.00131	37.4	-0.00158	24.5
			N = 15		Avg. Trend, % =		-78.9		-37.7		17.2		59.6

* Table 264 Smithsonian Physical Tables, 9th rev. ed., Washington DC, 1954.

** % Dev. = 100*(JT-pred - JT-meas)/JT-meas

Table 5. Summary of Overall Comparisons of the Experimental and Predicted Joule-Thomson Coefficients for Gaseous Nitrogen.

No. of Pts. Compared	Temp. Range deg. F	Pressure Psia	Orig. VDW Eqn. % Trend* in the JT Coeff.	API Soave % Trend* in the JT Coeff.	Redlich-Kwong % Trend* in the JT Coeff.	Peng-Robinson % Trend* in the JT Coeff.
16	minus 238 to 572	14.7	43.1	-30.6	6.8	18.3
16	minus 238 to 572	294	64.0	-36.6	12.5	20.9
15	minus 193 to 572	492	107.3	-57.1	23.3	27.4
15	minus 193 to 572	882	298.5	-153.7	77.0	60.8
15	minus 193 to 572	1470	110.1	-57.9	22.4	25.8
15	minus 193 to 572	2057	318.3	-186.8	69.7	72.6
15	minus 193 to 572	2645	55.9	-67.3	11.6	29.4
15	minus 193 to 572	2939	-78.9	-37.7	17.2	59.6
122			113.8	-77.7	29.7	39.0

* % Trend = Sum (% Dev)/N where % Dev = 100*(JT-pred. - JT-meas.)/JT-meas.

Data Source: "Smithsonian Physical Tables" Washington D.C. (1954).

Table 6. Comparison of Predicted and Experimental Joule-Thomson Coefficients for Gaseous Carbon Dioxide

Temp. deg. C	Temp. deg. F	Press. Atm	Press. Psia	Measured* JT Coeff. deg. C/Atm	Measured* JT Coeff. deg. F/Psia	Predicted JT Coeff. Orig. VDW Eqn. deg. F/Psia	% Dev**	Predicted JT Coeff. API Soave deg. F/Psia	% Dev**	Predicted JT Coeff. Redlich-Kwong deg. F/Psia	% Dev**	Predicted JT Coeff. Peng-Robinson deg. F/Psia	% Dev**
-50	-58	1	14.7	2.4130	0.2955	0.1303	-55.9	0.2336	-20.9	0.2047	-30.7	0.2359	-20.2
0	32	1	14.7	1.2900	0.1580	0.0965	-38.9	0.1587	0.5	0.1382	-12.5	0.1626	2.9
50	122	1	14.7	0.8950	0.1096	0.07467	-31.9	0.1129	3.0	0.0991	-9.6	0.1175	7.2
100	212	1	14.7	0.6490	0.0795	0.0596	-25.0	0.0828	4.2	0.0741	-6.8	0.0877	10.4
125	257	1	14.7	0.5600	0.0686	0.0538	-21.5	0.0716	4.4	0.0649	-5.4	0.0765	11.6
150	302	1	14.7	0.4890	0.0599	0.0488	-18.5	0.0621	3.7	0.0572	-4.5	0.0670	11.9
200	392	1	14.7	0.3770	0.0462	0.0407	-11.8	0.0473	2.5	0.0452	-2.1	0.0521	12.9
250	482	1	14.7	0.3075	0.0377	0.0344	-8.6	0.0363	-3.6	0.0364	-3.3	0.0410	8.9
300	572	1	14.7	0.2650	0.0324	0.0295	-9.1	0.0280	-13.7	0.0298	-8.2	0.0326	0.5
		N = 9		Avg. Trend, % =			-24.6		-2.2		-9.2		5.1
0	32	20	294	1.4020	0.1717	0.1122	-34.6	0.1710	-0.4	0.1511	-12.0	0.1747	1.8
50	122	20	294	0.8950	0.1096	0.0815	-25.6	0.1144	4.4	0.1026	-6.4	0.1186	8.2
100	212	20	294	0.6375	0.0781	0.0629	-19.4	0.0817	4.7	0.0748	-4.2	0.0861	10.3
125	257	20	294	0.5450	0.0667	0.0561	-15.9	0.0700	4.9	0.0650	-2.6	0.0745	11.6
150	302	20	294	0.4695	0.0575	0.0504	-12.3	0.0604	5.1	0.0569	-1.0	0.0649	12.9
200	392	20	294	0.3575	0.0438	0.0414	-5.4	0.0457	4.4	0.0446	1.9	0.0501	14.4
250	482	20	294	0.2885	0.0353	0.0347	-1.8	0.0349	-1.2	0.0357	1.1	0.0393	11.2
300	572	20	294	0.2425	0.0297	0.0295	-0.7	0.0269	-9.4	0.0291	-2.0	0.0311	4.7
		N = 8		Avg. Trend, % =			-14.5		1.5		-3.2		9.4
50	122	60	882	0.8800	0.1078	0.1042	-3.3	0.1115	3.5	0.1091	1.2	0.1138	5.6
100	212	60	882	0.6080	0.0744	0.0707	-5.0	0.0766	2.9	0.0746	0.2	0.0797	7.1
125	257	60	882	0.5160	0.0632	0.0610	-3.5	0.0650	2.9	0.0637	0.8	0.0683	8.1
150	302	60	882	0.4430	0.0542	0.0535	-1.4	0.0557	2.7	0.0552	1.8	0.0592	9.1
200	392	60	882	0.3400	0.0416	0.0426	2.3	0.0418	0.4	0.0427	2.6	0.0454	9.0
250	482	60	882	0.2625	0.0321	0.0350	8.9	0.0318	-1.1	0.0339	5.5	0.0355	10.4
300	572	60	882	0.2080	0.0255	0.0293	15.0	0.0245	-3.8	0.0275	8.0	0.0281	10.3
		N = 7		Avg. Trend, % =			1.9		1.1		2.9		8.5
50	122	73	1073.1	0.8225	0.1007	0.1149	14.1	0.1053	4.6	0.1080	7.2	0.1065	5.7
100	212	73	1073.1	0.5920	0.0725	0.0732	1.0	0.0738	1.8	0.0735	1.4	0.0765	5.5
125	257	73	1073.1	0.5068	0.0621	0.0624	0.6	0.0628	1.2	0.0627	1.0	0.0657	5.9
150	302	73	1073.1	0.4380	0.0536	0.0543	1.2	0.0539	0.5	0.0542	1.1	0.0570	6.3
200	392	73	1073.1	0.3325	0.0407	0.0427	4.9	0.0404	-0.8	0.0418	2.7	0.0437	7.3
250	482	73	1073.1	0.2565	0.0314	0.0349	11.1	0.0308	-1.9	0.0332	5.7	0.0342	8.9
300	572	73	1073.1	0.2002	0.0245	0.0291	18.7	0.0237	-3.3	0.0269	9.7	0.0271	10.5
		N = 7		Avg. Trend, % =			7.4		0.3		4.1		7.2

* Table 266 "Smithsonian Physical Tables," 9th rev. ed., Washington, D.C. 1954.

** % Dev = 100*(JT-pred. - JT-meas.)/JT-meas.

Table 6 (Cont.). Comparison of Predicted and Experimental Joule-Thomson Coefficients for Gaseous Carbon Dioxide

Temp. deg. C	Temp. deg. F	Press. Atm	Press. Psia	Measured* JT Coeff. deg. C/Atm	Measured* JT Coeff. deg. F/Psia	Predicted JT Coeff. Orig. VDW Eqn. deg. F/Psia	% Dev **	Predicted JT Coeff. API Soave deg. F/Psia	% Dev **	Predicted JT Coeff. Redlich-Kwong deg. F/Psia	% Dev **	Predicted JT Coeff. Peng-Robinson deg. F/Psia	% Dev **
50	122	100	1470	0.5570	0.0682	0.0567	-16.9	0.0659	-3.4	0.0646	-5.3	0.0658	-3.5
100	212	100	1470	0.5405	0.0662	0.0755	14.1	0.0661	-0.1	0.0686	3.7	0.0677	2.3
125	257	100	1470	0.4750	0.0582	0.0636	9.3	0.0572	-1.7	0.0591	1.6	0.0592	1.8
150	302	100	1470	0.4155	0.0509	0.0548	7.7	0.0494	-2.9	0.0513	0.8	0.0518	1.8
200	392	100	1470	0.3150	0.0386	0.0425	10.2	0.0374	-3.0	0.0397	2.9	0.0402	4.2
250	482	100	1470	0.2420	0.0296	0.0344	16.1	0.0286	-3.5	0.0315	6.3	0.0316	6.6
300	572	100	1470	0.1872	0.0229	0.0286	24.8	0.0220	-4.0	0.0255	11.2	0.0251	9.5
		N = 7	Avg. Trend, % =				9.3		-2.7		3.0		3.2
50	122	140	2058	0.1720	0.0211	0.0155	-26.4	0.0243	15.4	0.0220	4.5	0.0246	16.8
100	212	140	2058	0.4320	0.0529	0.0530	0.2	0.0505	-4.5	0.0522	-1.3	0.0511	-3.4
125	257	140	2058	0.4130	0.0506	0.0548	8.4	0.0470	-7.1	0.0494	-2.3	0.0480	-5.1
150	302	140	2058	0.3760	0.0460	0.0502	9.0	0.0420	-8.8	0.0446	-3.1	0.0435	-5.5
200	392	140	2058	0.2890	0.0354	0.0402	13.6	0.0328	-7.3	0.0356	0.6	0.0349	-1.4
250	482	140	2058	0.2235	0.0274	0.0326	19.1	0.0254	-7.2	0.0286	4.5	0.0278	1.6
300	572	140	2058	0.1700	0.0208	0.0271	30.2	0.0197	-5.4	0.0233	11.9	0.0223	7.1
		N = 7	Avg. Trend, % =				7.7		-3.6		2.1		1.4
50	122	180	2646	0.1025	0.0126	0.00536	-57.3	0.0143	13.9	0.0122	-2.8	0.0147	17.1
100	212	180	2646	0.3000	0.0367	0.0245	-33.3	0.0351	-4.5	0.0330	-10.2	0.0354	-3.6
125	257	180	2646	0.3230	0.0396	0.0335	-15.3	0.0364	-8.0	0.0367	-7.2	0.0370	-6.4
150	302	180	2646	0.3102	0.0380	0.0371	-2.3	0.0344	-9.4	0.0359	-5.5	0.0353	-7.1
200	392	180	2646	0.2600	0.0318	0.0345	8.4	0.0282	-11.4	0.0307	-3.6	0.0297	-6.7
250	482	180	2646	0.2045	0.0250	0.0293	17.0	0.0223	-10.9	0.0254	1.4	0.0243	-3.0
300	572	180	2646	0.1540	0.0189	0.0248	31.5	0.0175	-7.2	0.0210	11.4	0.0197	4.5
		N = 7	Avg. Trend, % =				-7.3		-5.4		-2.3		-0.7
50	122	200	2940	0.0930	0.0114	0.00257	-77.4	0.0116	1.9	0.00956	-16.1	0.0120	5.4
100	212	200	2940	0.2555	0.0313	0.0168	-46.3	0.0290	-7.3	0.0260	-16.9	0.0294	-6.0
125	257	200	2940	0.2915	0.0357	0.0246	-31.1	0.0316	-11.5	0.0307	-14.0	0.0321	-10.1
150	302	200	2940	0.2910	0.0356	0.0297	-16.6	0.0308	-13.6	0.0315	-11.6	0.0316	-11.3
200	392	200	2940	0.2455	0.0301	0.0307	2.1	0.0260	-13.5	0.0281	-6.5	0.0273	-9.2
250	482	200	2940	0.1975	0.0242	0.0272	12.5	0.0209	-13.6	0.0237	-2.0	0.0226	-6.5
300	572	200	2940	0.1505	0.0184	0.0234	27.0	0.0164	-11.0	0.0197	6.9	0.0185	0.4
		N = 7	Avg. Trend, % =				-18.6		-9.8		-8.6		-5.3

* Table 266 "Smithsonian Physical Tables," 9th rev. ed., Washington, D.C. 1954.

** % Dev = 100*(JT-pred - JT-meas)/JT-meas

Table 7. Summary of Overall Comparisons of the Experimental and Predicted Joule-Thomson Coefficients for Gaseous Carbon Dioxide.

No. of Pts. Compared	Temp. Range deg. F	Pressure Psia	Orig. VDW Eqn. % Trend* in the JT Coeff.	API Soave % Trend* in the JT Coeff.	Redlich-Kwong % Trend* in the JT Coeff.	Peng-Robinson % Trend* in the JT Coeff.
9	minus 58 to 572	14.7	-24.6	-2.2	-9.2	5.1
8	32 to 572	294	-14.5	1.5	-3.2	9.4
7	122 to 572	882	1.9	1.1	2.9	8.5
7	122 to 572	1073.1	7.4	0.3	4.1	7.2
7	122 to 572	1470	9.3	-2.7	3.0	3.2
7	122 to 572	2058	7.7	-3.6	2.1	1.4
7	122 to 572	2646	-7.3	-5.4	-2.3	0.7
7	122 to 572	2940	-18.6	-9.8	-8.6	-5.3
59			-5.7	-2.5	-1.7	3.9

* % Trend = Sum (% Dev)/N where % Dev = 100*(JT-pred. - JT-meas.)/JT-meas.

Data Source: "Smithsonian Physical Tables" Washington D.C. (1954).

Table 8. Comparison of Predicted and Experimental Joule-Thomson Coefficients for Liquid Carbon Dioxide.

Temp. deg. C	Temp. deg. F	Press. Atm	Press. Psia	Measured* JT Coeff. deg. C/Atm	Measured* JT Coeff. deg. F/Psia	Predicted JT Coeff. Orig. VDW Eqn. deg. F/Psia	Abs % Dev **	Predicted JT Coeff. API Soave deg. F/Psia	Abs % Dev **	Predicted JT Coeff. Redlich-Kwong deg. F/Psia	Abs % Dev **	Predicted JT Coeff. Peng-Robinson deg. F/Psia	Abs % Dev **
-75	-103	20	294	-0.0200	-0.0024	-0.00859	250.8	-0.00285	16.4	-0.0023	6.1	-0.00278	13.5
-50	-58	20	294	-0.0140	-0.0017	-0.00378	120.5	-0.00115	32.9	-0.00073	57.4	-0.00118	31.2
-75	-103	60	882	-0.0200	-0.0024	-0.00978	299.4	-0.00304	24.1	-0.00252	2.9	-0.00294	20.1
-50	-58	60	882	-0.0150	-0.0018	-0.00631	243.5	-0.00156	15.1	-0.00127	30.9	-0.00152	17.2
0	32	60	882	0.0370	0.0045	0.0122	169.3	0.00694	53.2	0.00825	82.1	0.00655	44.6
-75	-103	73	1073.1	-0.0232	-0.0028	-0.0101	255.5	-0.00310	9.1	-0.00259	8.8	-0.00298	4.9
-50	-58	73	1073.1	-0.0165	-0.0020	-0.00692	242.5	-0.00168	16.8	0.00142	170.3	-0.00162	19.8
0	32	73	1073.1	0.0310	0.0038	0.00772	103.4	0.00600	58.1	0.00682	79.7	0.00572	50.7
-75	-103	100	1470	-0.0228	-0.0028	-0.0107	283.3	-0.00321	15.0	-0.00271	2.9	-0.00308	10.3
-50	-58	100	1470	-0.0160	-0.0020	-0.00795	305.8	-0.00190	3.0	-0.0017	13.2	-0.00182	7.1
0	32	100	1470	0.0215	0.0026	0.00226	14.2	0.00447	69.8	0.00469	78.1	0.00436	65.6
-75	-103	140	2058	-0.0240	-0.0029	-0.0113	284.5	-0.00336	14.3	-0.00288	2.0	-0.00321	9.2
-50	-58	140	2058	-0.0183	-0.0022	-0.00910	306.1	-0.00220	1.8	-0.00205	8.5	-0.00208	7.2
0	32	140	2058	0.0115	0.0014	-0.00210	249.1	0.00287	103.8	0.00263	86.8	0.00291	106.7
-75	-103	180	2646	-0.0250	-0.0031	-0.0119	288.7	-0.00350	14.3	-0.00302	1.3	-0.00333	8.8
-50	-58	180	2646	-0.0228	-0.0028	-0.00997	257.1	-0.00245	12.2	-0.00234	16.2	-0.00230	17.6
0	32	180	2646	0.0085	0.0010	-0.00464	545.8	0.00173	66.2	0.00125	20.1	0.00185	77.7
-75	-103	200	2940	-0.0290	-0.0036	-0.0121	240.7	-0.00356	0.3	-0.00309	13.0	-0.00338	4.8
-50	-58	200	2940	-0.0248	-0.0030	-0.0103	239.2	-0.00257	15.4	-0.00247	18.7	-0.00240	21.0
0	32	200	2940	0.0045	0.0006	-0.00557	1110.9	0.00126	128.7	0.000717	30.1	0.00142	157.7
N = 20 bs Avg Dev, % (Overall) =							290.5		33.5		36.5		34.8

* Table 266 "Smithsonian Physical Tables," 9th rev. ed., Washington, D.C. 1954.

** Abs % Dev = 100*ABS((Pred - Meas)/Meas)